TECHNISCHE UNIVERSITÄT MÜNCHEN

UNC production and loss cross sections in cryogenic converters (D2 and O2), deduced from neutron scattering experiments, and comparison with direct UCN production experiments

E. Gutsmiedl[1], A.R. Müller, A. Frei, S. Paul, M. Urban, F. Böhle, A. Maier, R. Bozhanova, S. Wlokka, C. Morkel[2], J. Klenke[4] ,H. Schober[3], A. Orecchini[3], S. Rols[3], T. Unruh[5]

1] Physik Department E18, TU Munich

2] Physik Department, E21, TU Munich

3] Institut Laue-Langevin Grenoble

4] FRM II, TU Munich

5] Universität Erlangen , Germany

NEUTRONS FOR SCIENCE

Institut Laue-Langevin

LMU Excellence Cluster Universe

Scope

- Motivation
- Neutron scattering techniques
- Neutron scattering in sD_2
- Neutron scattering in sO_2
- Summary

Motivation:

Why do we need strong sources of Ultra-Cold-Neutrons (UCN)?

Answer: UCN are suitable particles for studies of fundamental questions

- Physical properties of the neutron itself
  a) neutron lifetime
  b) neutron electric dipole moment

- UCN as quantum objects for testing the „Schrödinger equation"
  a) quantum states in a gravitational field
  b) neutron optics (interference effects)

Advantages:
- UCN can be stored in in material and magnetic bottles
- Long observations times (few thousand seconds)
- Easy to polarize (spin) and keep the polarization

Disadvantages:
- UCN absorbtion cross section (1/v law)
- UCN up-scattering

Superthermal UCN production

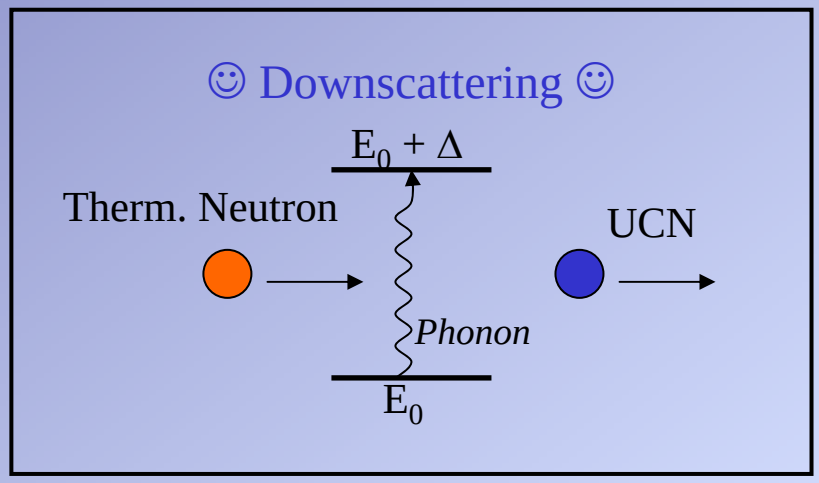

- Inelastic scattering:
  - Production: $E_{UCN} + \Delta \rightarrow E_{UCN}$ (Downscattering)
  - Loss process: $E_{UCN} \rightarrow E_{UCN} + \Delta$ (Upscattering)

- Principle of detailed balance:

$$\sigma_{up} = \frac{E_{UCN} + \Delta}{E_{UCN}} \cdot e^{-\Delta / k_B T} \cdot \sigma_{down}$$

- For $\Delta >> k_B T >> E_{UCN} \Rightarrow \sigma_{up} << \sigma_{down} \Rightarrow$ **Superthermal Source**

Neutron scattering - basics

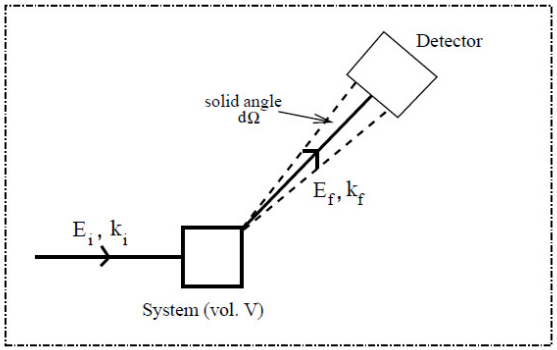

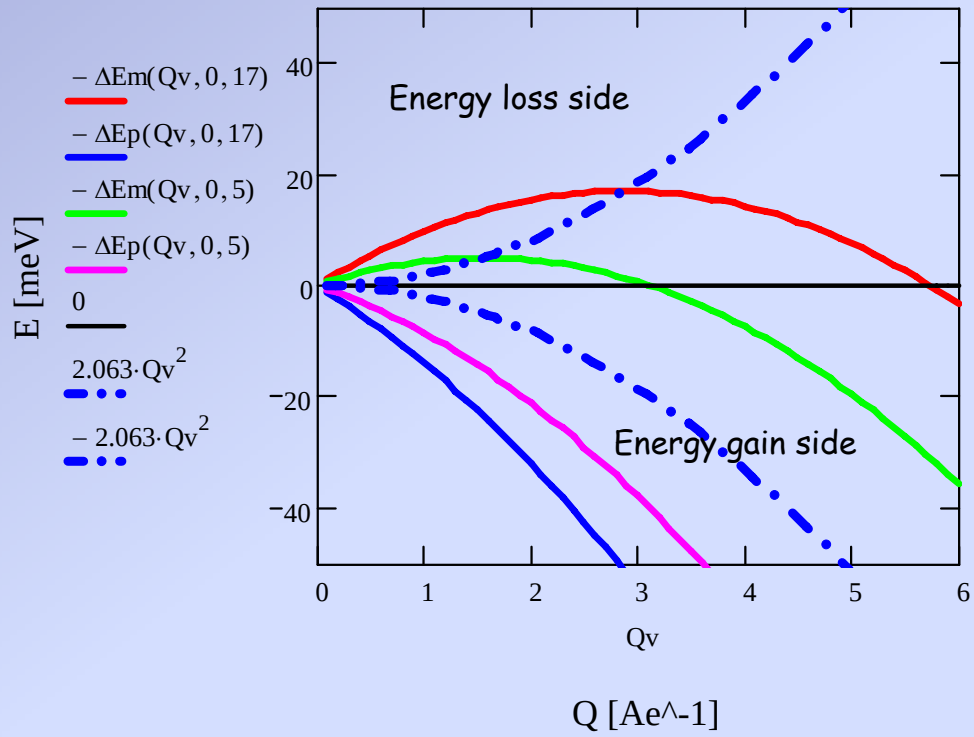

Q [Ae^-1]

$$\frac{d^2\sigma}{dEd\Omega} = \frac{k_f}{k_i} b^2(Q) S(Q,E)$$

Scattering experiments give direct information on space and time-dependent correlations in the system.

$$E = E_f - E_i$$
$$\vec{Q} = \vec{k_f} - \vec{k_i}$$

Kinematics
UCN production and losses

UCN production:

$$E = E_f - E_i; E_f \ll E_i \rightarrow E \simeq E_i$$

$$\vec{Q} = \vec{k_f} - \vec{k_i}; \mid \vec{k_f} \mid \ll \mid \vec{k_i} \mid \rightarrow \mid \vec{Q} \mid \simeq \mid \vec{k_i} \mid$$

$$\sigma_{\mathrm{UCN}}(E_0) = \frac{\sigma_0}{k_0} S(k_0, \frac{\hbar^2}{2m} k_0^2) \frac{2}{3} k_{\mathrm{U}}^{\max} E_{\mathrm{U}}^{\max}.$$

UCN losses:

$$E = E_f - E_i; E_i \ll E_f \rightarrow E \simeq E_f$$

$$\vec{Q} = \vec{k_f} - \vec{k_i}; \mid \vec{k_f} \mid \gg \mid \vec{k_i} \mid \rightarrow \mid \vec{Q} \mid \simeq \mid \vec{k_f} \mid$$

$$\sigma_{\mathrm{loss}}(k_i) = \sigma_0 \cdot \frac{2}{k_i} \cdot \int_0^{Q^{\max}} \frac{\hbar^2 Q^2}{2m} S(Q, \frac{\hbar^2 Q^2}{2m}) dQ + \sigma_{inc}^{el}.$$

$$\sigma_{\mathrm{loss}}(E_i) = \frac{\sigma_0}{\sqrt{\frac{\hbar^2 E_i}{2m}}} \cdot \int_0^{E^{\max}} \sqrt{\frac{2mE}{\hbar^2}} S(\frac{2mE}{\hbar^2}, E) dE + \sigma_{inc}^{el}.$$

Neutron scattering in sD_2:

Experiments:

TOFTOF FRM II

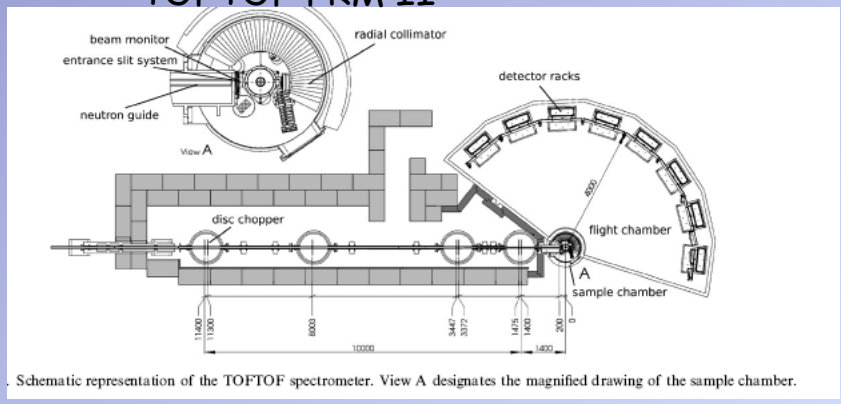

Schematic representation of the TOFTOF spectrometer. View A designates the magnified drawing of the sample chamber.

TOFTOF. Forschungsneutronenquelle Heinz Maier-Leibnitz (FRM II)

Anzahl der Chopperscheiben

7

Chopper Drehzahl

1000 1/min - 22000 1/min

Scheibendurchmesser

600 mm

Weite des Neutronenleiters am Instrument Eingang

44 x 100 mm^2

Weite des Neutronenleiters an der Probenposition

23 x 47 mm^2

einfallende Wellenlänge

1.5 - 16 Ångström

elastische Energieauflösung

5 µeV - 5 meV

Energieübertragung

-10 meV - 50 meV

gesammte Durchflussmenge des weißen Strahls an der Probenposition

1 x 10^{10} $n/cm^2/s$

Winkelbereich der Detektorbank

-15° bis -7° und 7° bis 140°

subthermal neutrons
E_0 ~ 12 meV
ΔE_R=0.63 meV

IN 4 ILL Grenoble

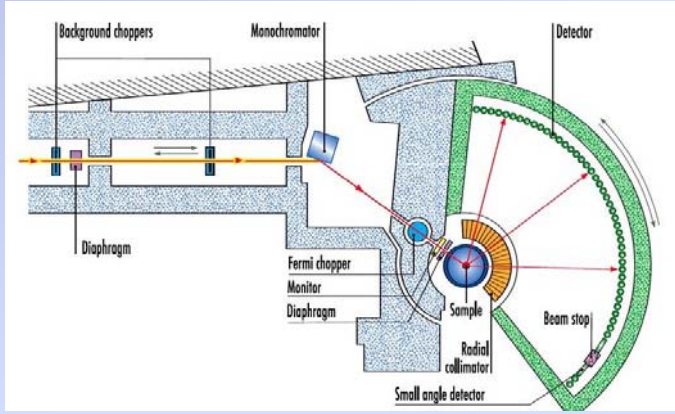

Instrument description

Reactor hall, thermal beam H12	
Monochromators	
PG 002: 2.20 ... 3.60 Å PG 004: 1.10 ... 1.80 Å Cu 220: 0.85 ... 1.50 Å *(summer 2005)* *Cu 111: 1.25 ... 2.24 Å*	
take-off angle 2θM	39 ° ... 65°
resolution $\delta > E_i / E_i$	3 ... 6 %
flux on sample	5 x 10^5 $cm^{-2}s^{-1}$
background choppers v_{max}	5 000 rpm
Fermi chopper v_{max}	32 000 rpm
duty cycle	3 x 10^{-3}
beam size on sample	2 x 4 cm^2
primary collimation δθ	1°

Thermal neutrons
E_0 ~ 17 meV
ΔE_R=0.7 meV

TOFTOF-sample stick

D_2 sample cell

Solid D_2

Liquid => Solid (quick & dirty)

Gas => Solid (T < 10K)

Freezing D_2

from gas (at T~16 - 17 K)

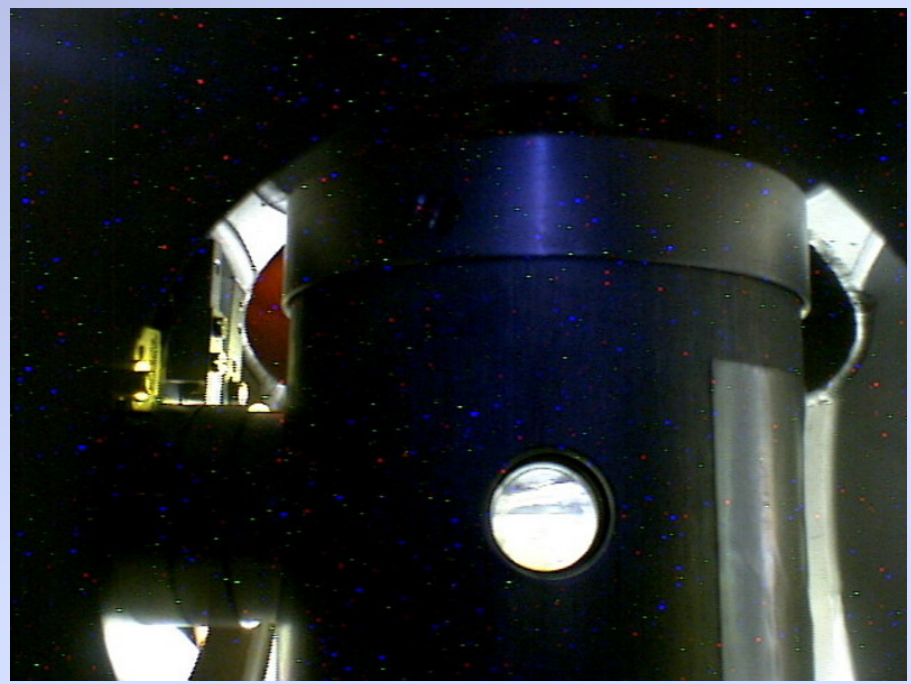

Para – and ortho-D_2

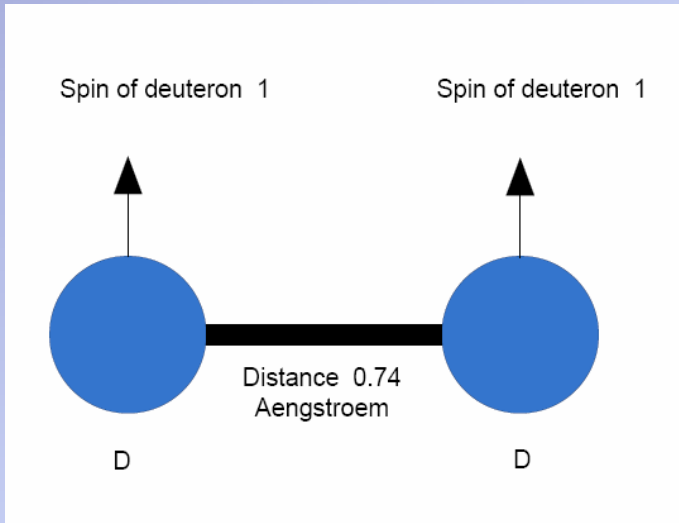

Combination of spin's leads to ID_2= 0; 1; 2
Ortho-D_2 : ID_2= 0; 2 (symmetric wave function -> J is even)
Para-D_2 : ID_2= 1 (anti-symmetric wave function -> J is odd)

$$E_J = k_B \cdot \{B_v J(J+1) - D_e J^2 (J+1)^2\}$$

E_1~ 7.4 meV

$$c_g = \frac{g_e}{Z} \sum_{J=0,2,\ldots} (2J+1) \exp\left(\frac{-E_J}{k_B T}\right)$$

$$c_u = \frac{g_u}{Z} \sum_{J=1,3,\ldots} (2J+1) \exp\left(\frac{-E_J}{k_B T}\right)$$

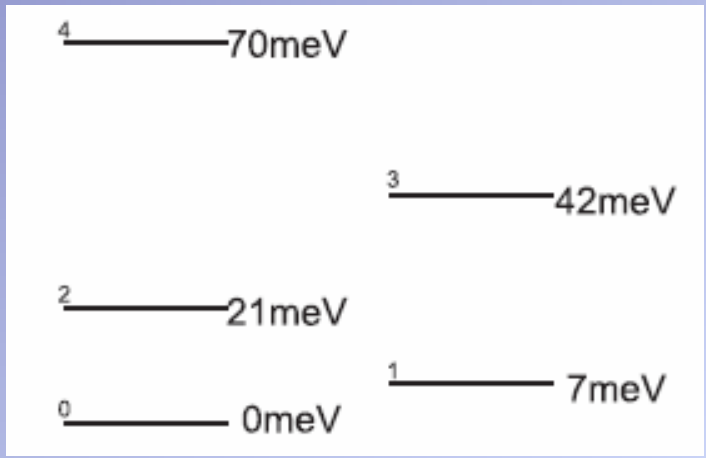

J=1 ground state of para D_2

J=0 ground state of ortho D_2

Para-Ortho-Conversion:
- Magnetic dipole interaction between molecules
- Interaction of nuclear quadrupole moment of one D2 molecule with the total quadrupole moment of a other D2 molecule

The most outstanding property of solid H_2, HD and D_2 is that the rotational motion of the molecules in these crystals is free in the sense that the rotational quantum number, J, is a very good quantum number. The anisotropic intermolecular forces in these crystals are weak compared to the energy separations between the different rotational states, and these forces therefore do not mix appreciably states corresponding to different values of J. Similar remarks apply to the internal vibrational motion of the molecules characterized by the vibrational quantum number v.

I. van Kranendonk and V.F. Sears Can. J. Phys, 44, 313 (1966)

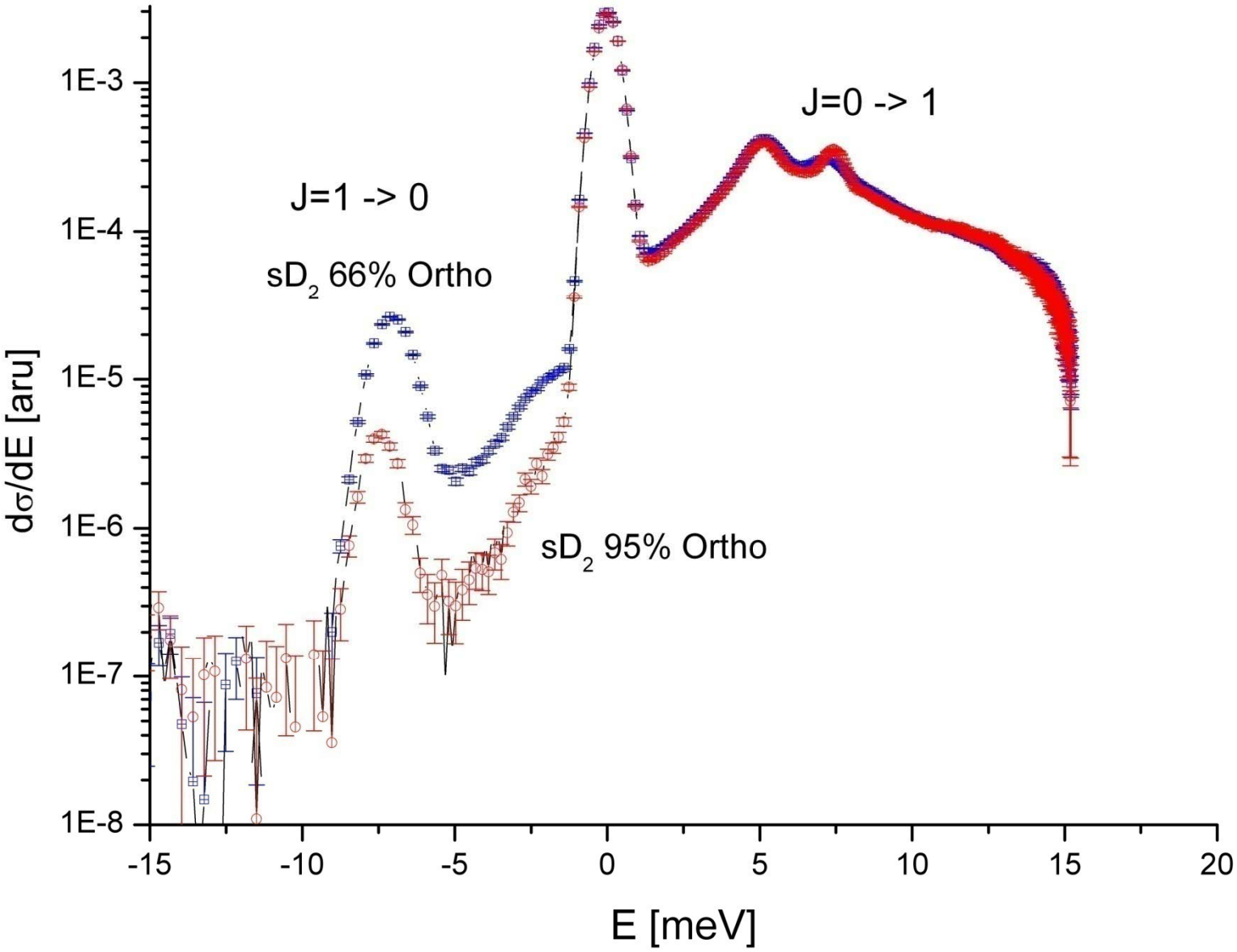
J=0 -> 1
J=1 -> 0
sD2 66% Ortho
sD2 95% Ortho
dσ/dE [aru]
1E-3
1E-4
1E-5
1E-6
1E-7
1E-8
-15
-10
-5
0
5
10
15
20
E [meV]

Dynamics

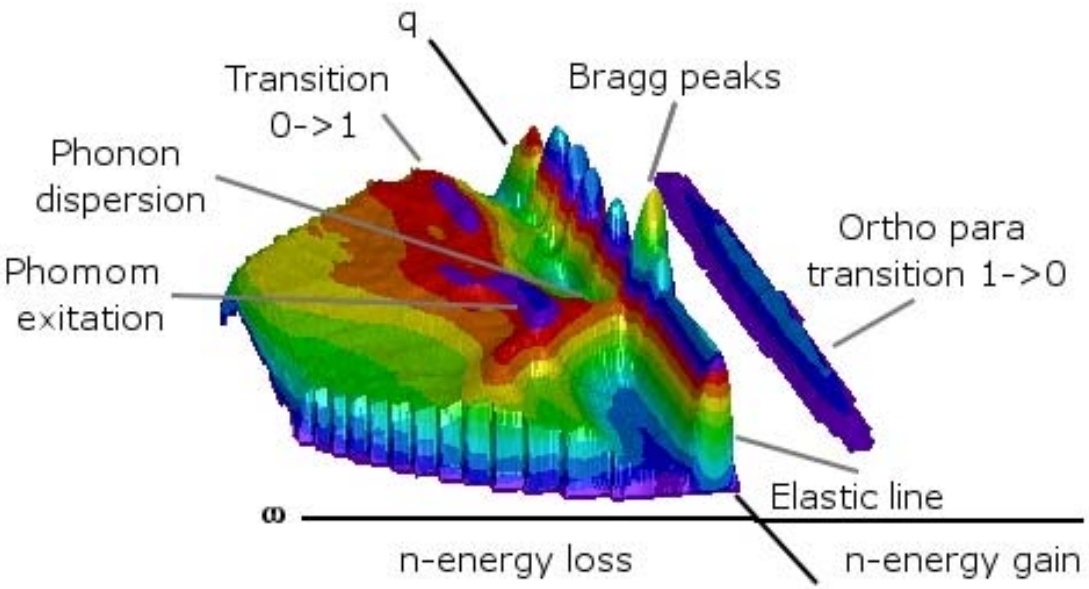
q
Transition
0->1
Bragg peaks
Phonon
dispersion
Ortho para
transition 1->0
Phomom
exitation
Elastic line
ω
n-energy loss
n-energy gain

Static structure:

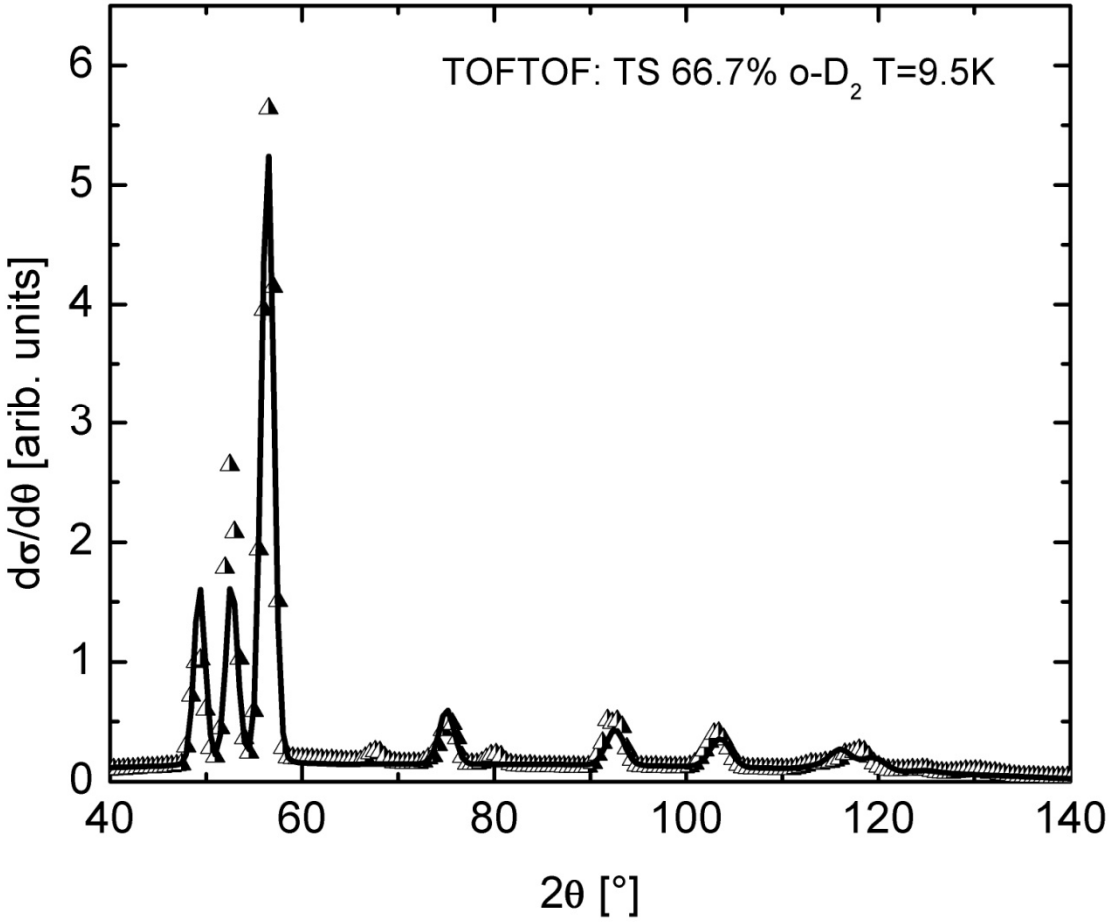

hcp structure

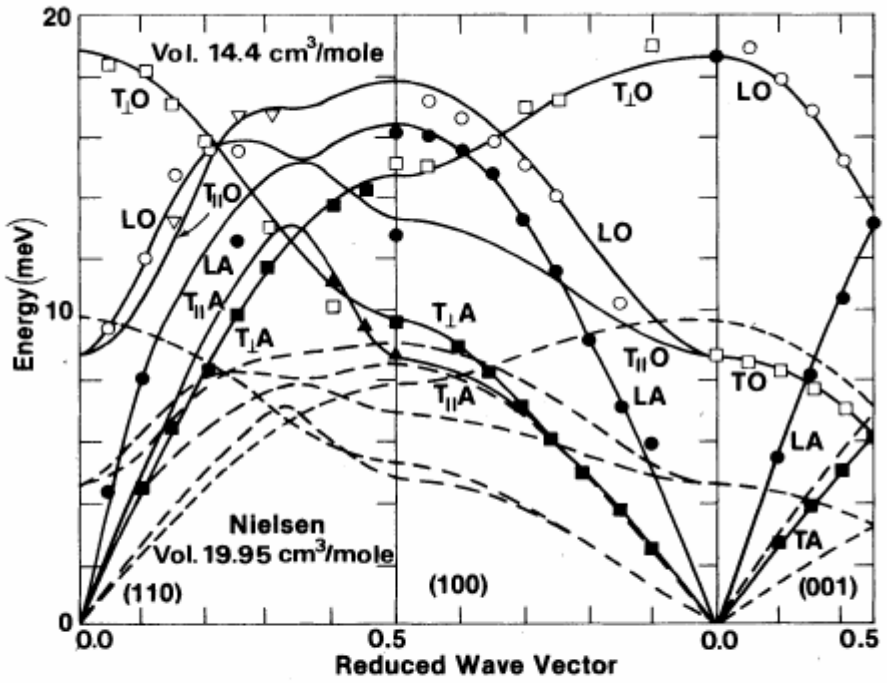

FIG. 4. Dispersion curve for hcp orthodeuterium showing energy shifts with density increase. Solid curve, 14.4 cm^3/mole; dashed curve, low pressure, molar volume 19.95 cm^3/mole (Ref. 11).

J.W. Schmidt et al. PRB 30, 6308 (1984)

Generalized density of states (GDOS):

sD_2 from liquid phase – 66.7% Ortho

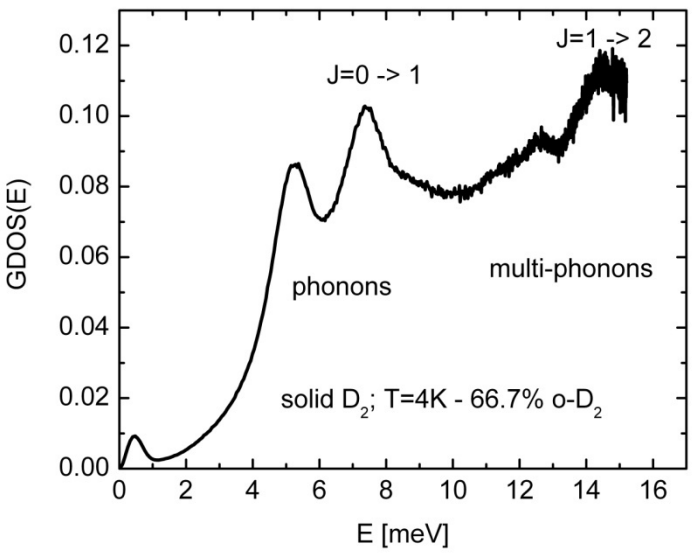

sD_2 from liquid phase - 95% Ortho

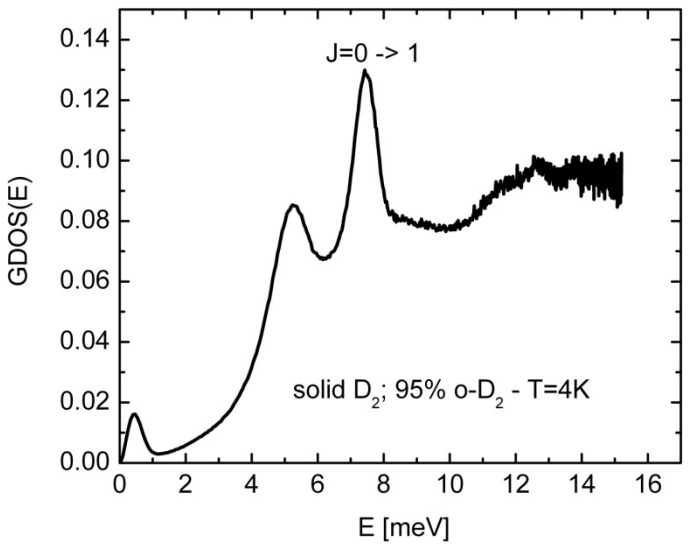

Density of states from measurements

Z-Ch. Yu, S.S. Malik, R. Golub, Z. Phys. B - Condensed Matter **62** (1986) 137

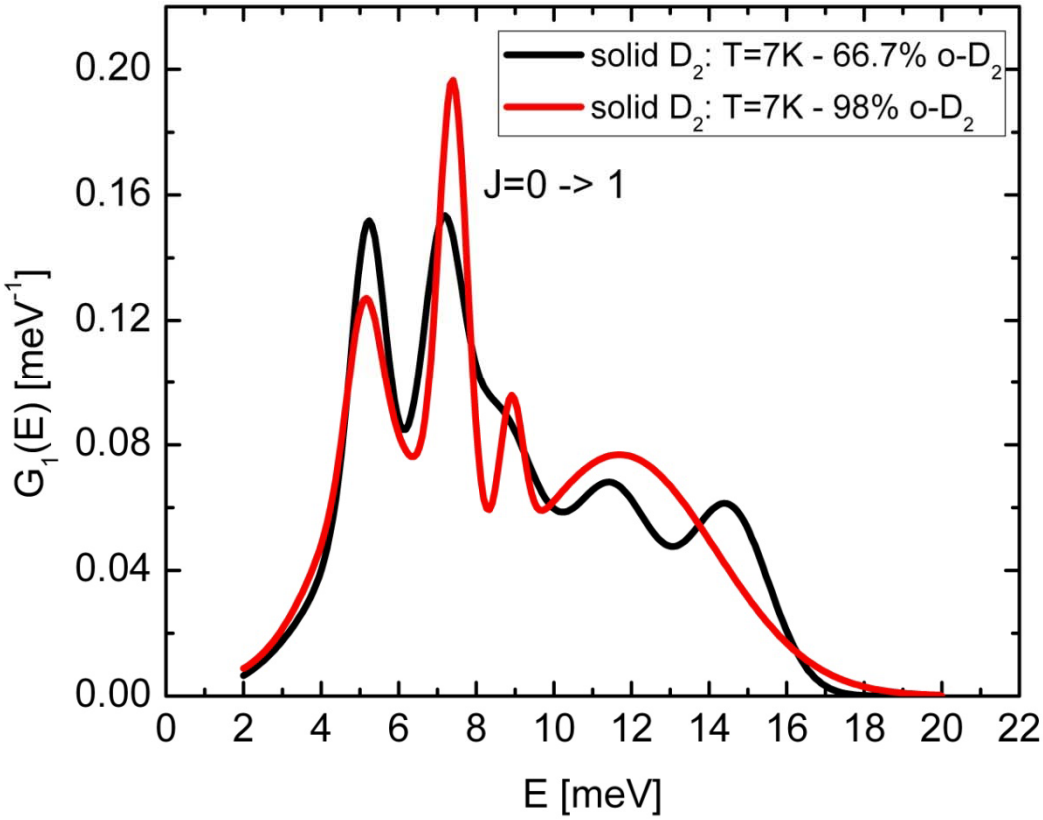

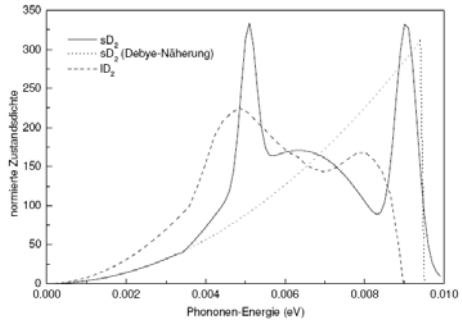

Direct determination of UCN production cross section

$$\sigma_{\mathrm{UCN}}(E) = \frac{\sigma_0}{k} S(k, \frac{\hbar^2}{2m}k^2)\frac{2}{3}k_{\mathrm{U}}^{\max}E_{\mathrm{U}}^{\max}.$$

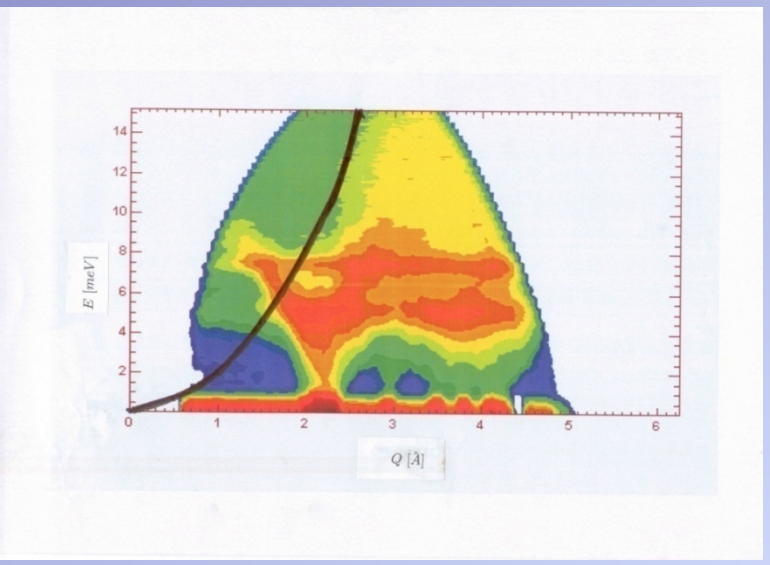

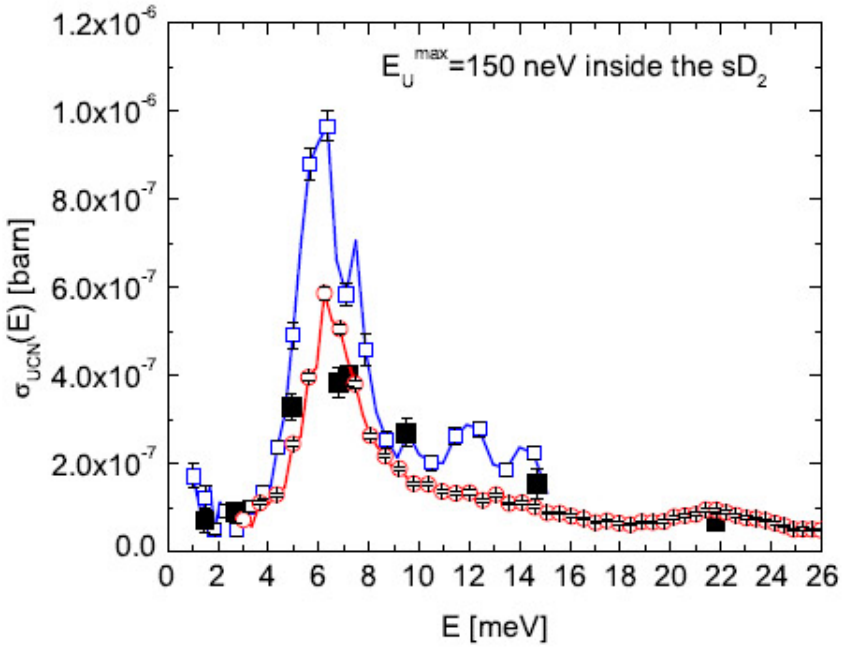

Production rate:
T_n=40K ;
P_{UCN}= 6.6 10^5 cm^{-3} s^{-1}

$$P_{\mathrm{UCN}}(T_{\mathrm{n}}) = N_{\mathrm{D_2}} \cdot \int_0^{E^{\max}} \frac{d\Phi(T_n)}{dE_0} dE_0 \cdot \sigma_{UCN}(E_0).$$

$$\rho_{UCN} = P_{UCN} \cdot \tau_{UCN} \ [cm^{-3}]$$

UCN production at the FRM II MEPHISTO-beam
Cold flux ~ 5 10^9 cm^{-2} s^{-1}

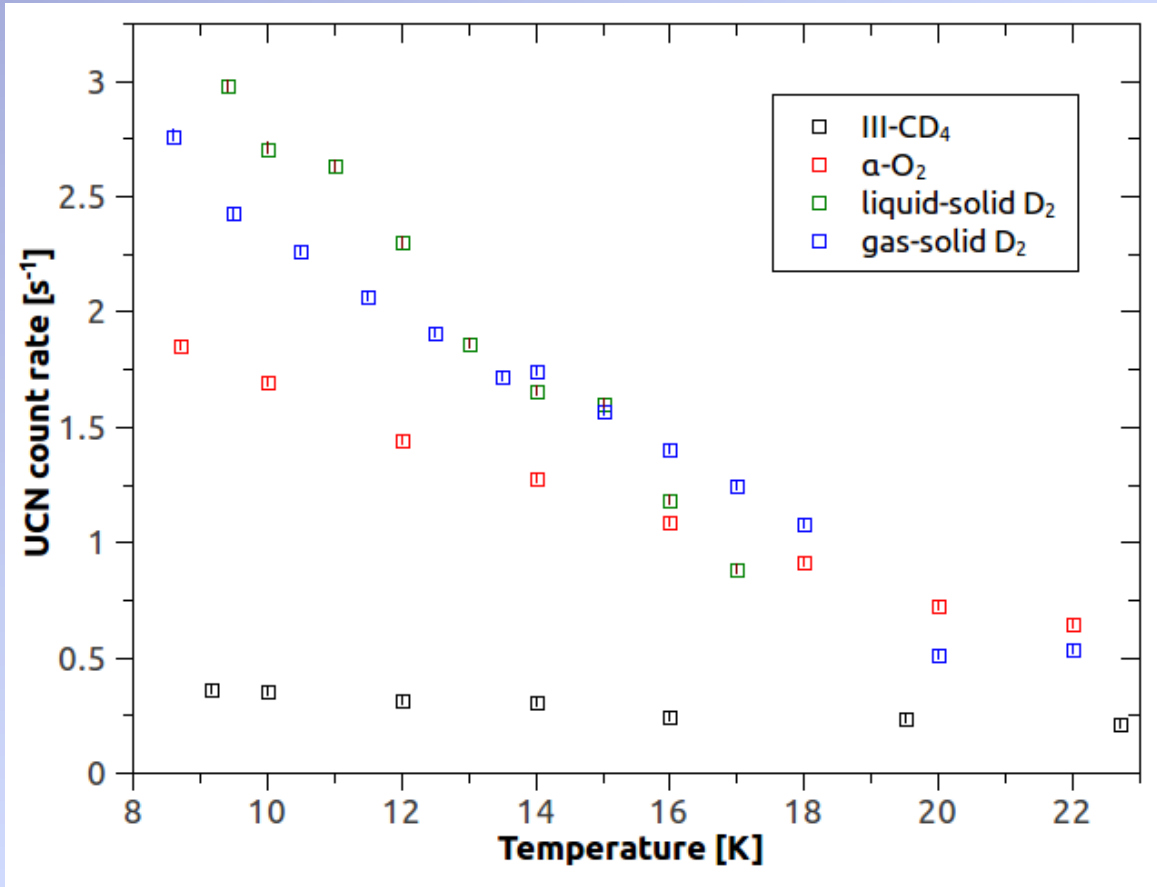

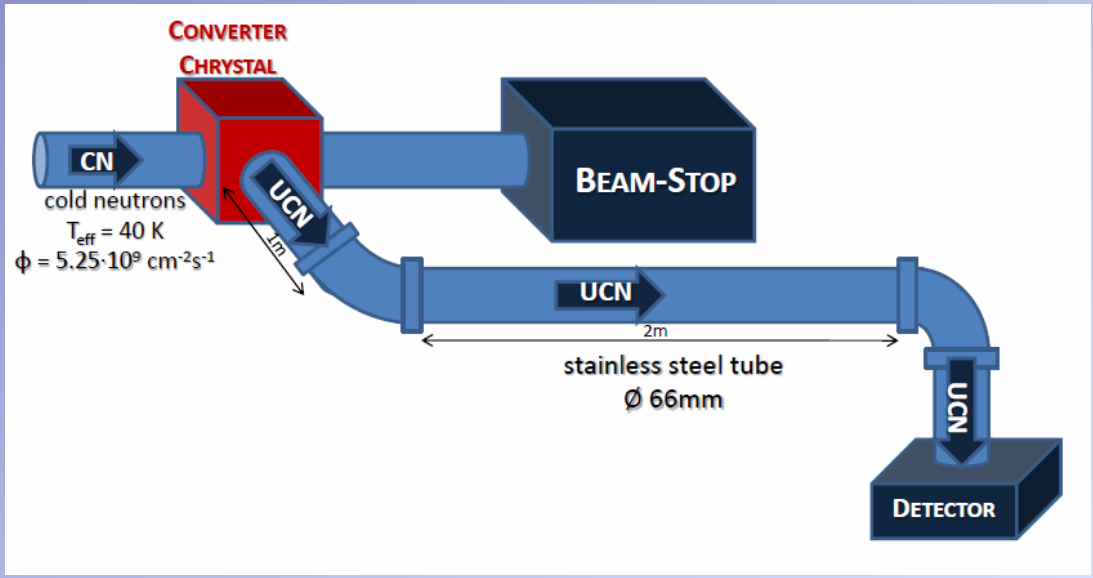
CONVERTER
CHRYSTAL
CN
cold neutrons
T_{eff} = 40 K
$\phi = 5.25 \cdot 10^9$ cm^{-2}s^{-1}
UCN
1m
BEAM-STOP
UCN
2m
stainless steel tube
Ø 66mm
UCN
DETECTOR

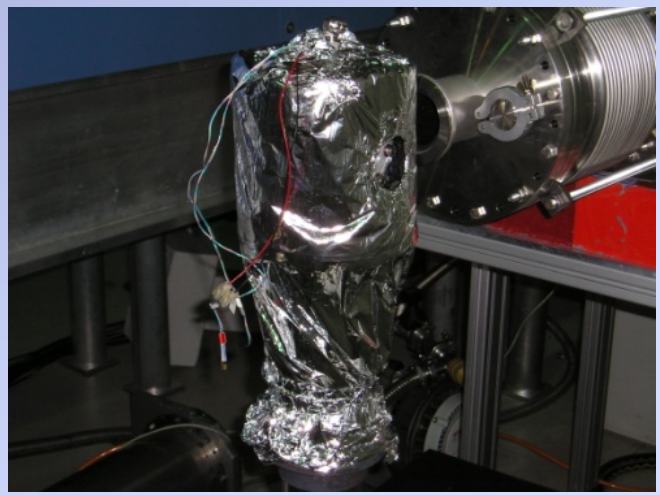

Calibration of cross section

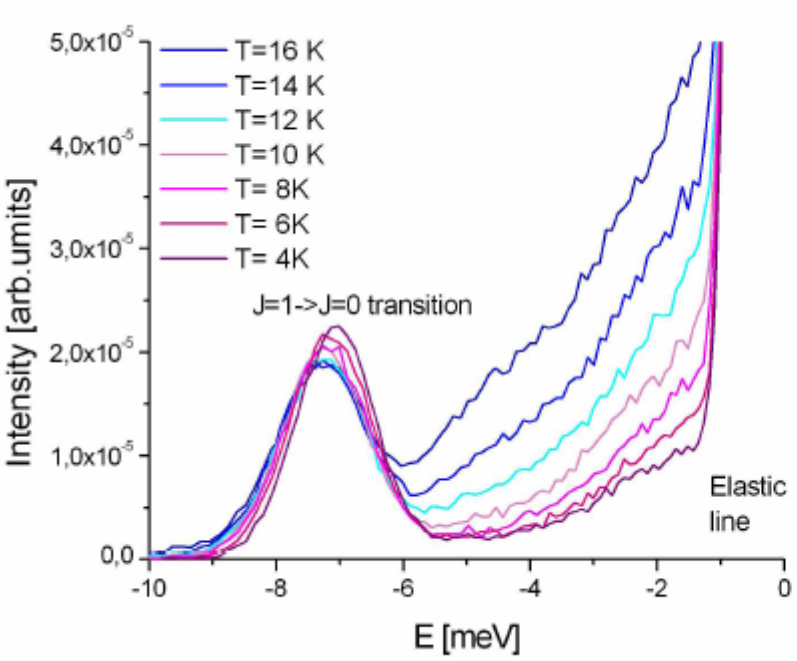

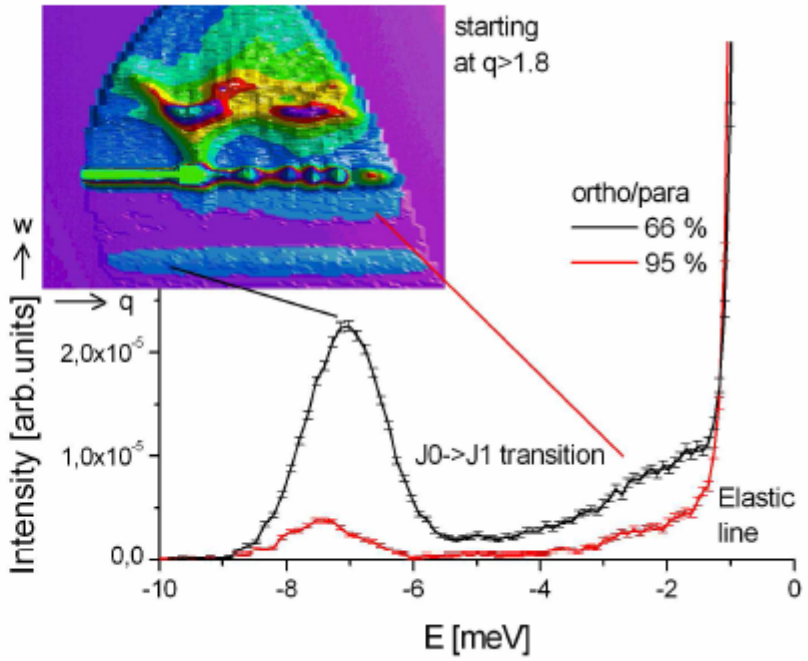

σ–up (J=1->0)=0.029 barn for E_i=17.2 meV neutrons

M. Hamermesh and J. Schwinger PR 69, (1946) 145

σ_{tot} =23.4 barn --- σ_{tot} (TURCHIN)=23.8 barn

W.E. Lamb, PR 55, (1939) 190

UCN losses ?

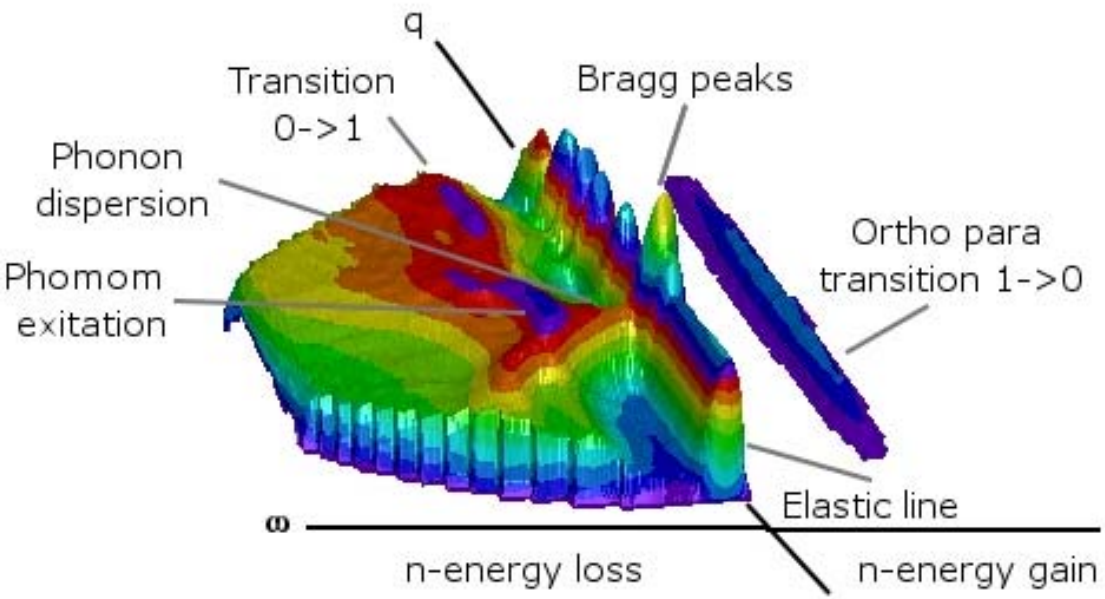
q
Transition
0->1
Bragg peaks
Phonon
dispersion
Ortho para
transition 1->0
Phomom
exitation
Elastic line
ω
n-energy loss
n-energy gain

Experimental results on UCN production :

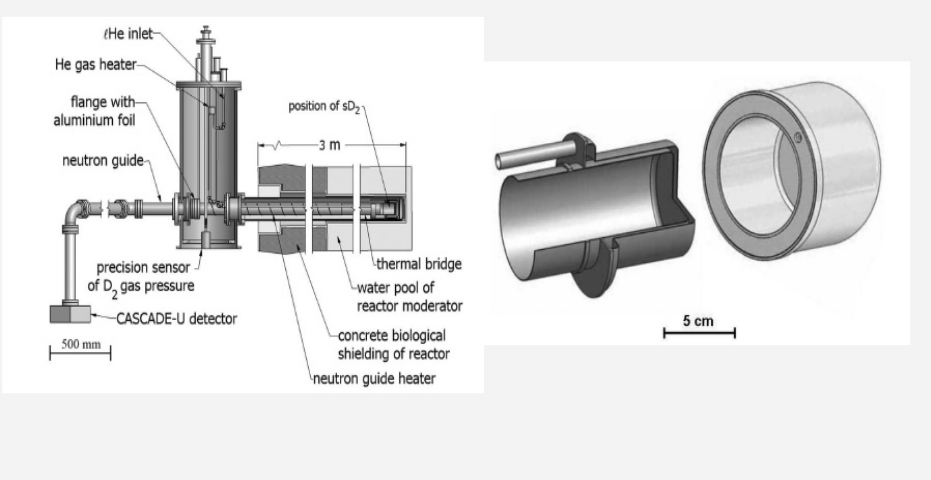

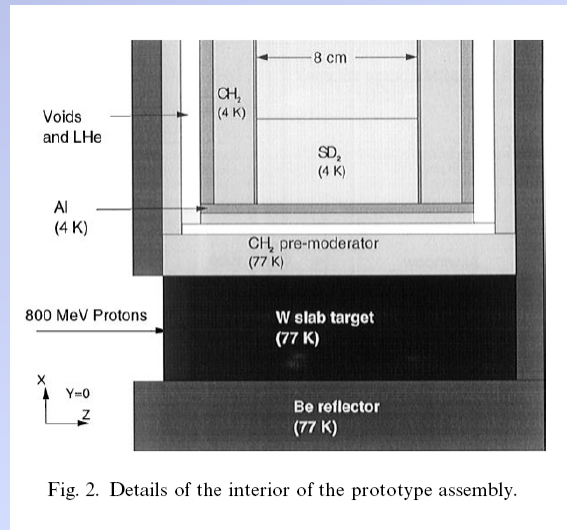

Fig. 2. Details of the interior of the prototype assembly.

Triga Mainz Experiments

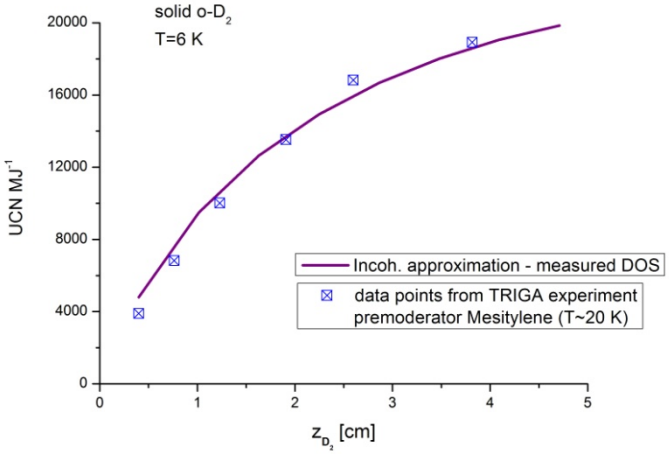

$$I(x) := I0 \cdot \left(1 - e^{\frac{-x}{\lambda}}\right)$$

$\lambda \sim 2$ cm

$\sigma_{loss} \sim 16$ barn - $v_U \sim 3.2$ m/s

$\sigma_a + \sigma_p \sim 4.2$ barn

$\sigma_{1P}^{up} \sim 1.4$ barn

$\sigma_{inc} \sim 5$ barn

LANL Experiments

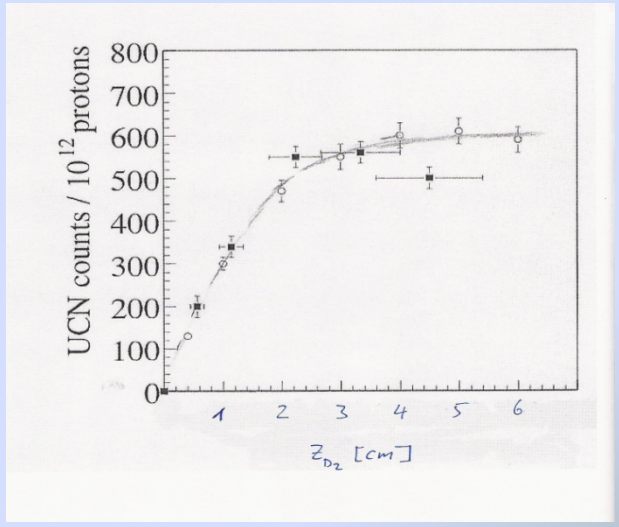

Temperature dependance of UCN yield

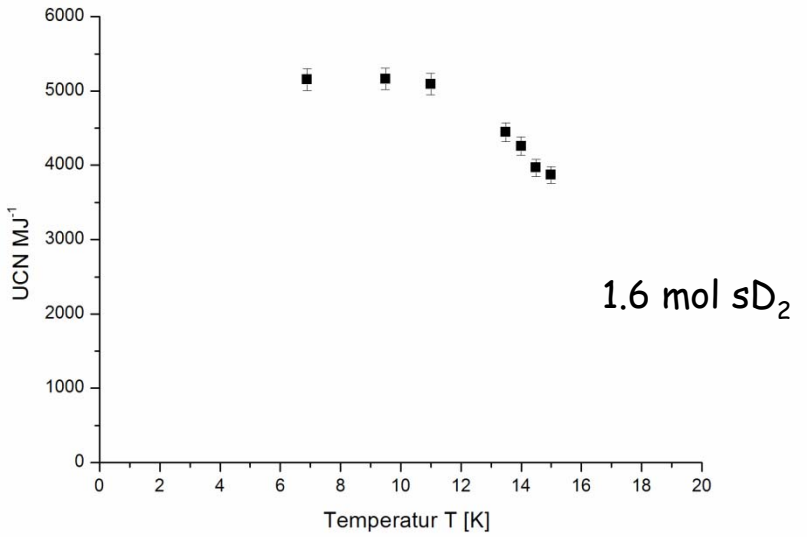

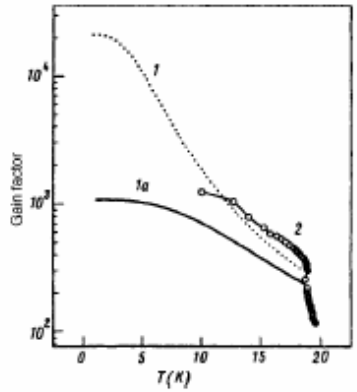

FIG. 2. Temperature gain of UCN yield for solid deuterium normalized to the UCN yield at room temperature: *1* — Computed curve for a large source with incoherent elastic scattering cross section of UCNs equal to zero or for a UCN source in the accumulation mode; *1a* — computed curve for a large source taking account of UCN scattering (2.2 b) and the hydrogen impurity (0.2%); *2* — experimental results obtained on a reactor with a source volume of 6 liters of solid deuterium containing 0.2% hydrogen. The large increase in the UC yield at 18.7 K is due to a transition from the liquid to the solid state.

TRIGA experiment

Serebrov et al.

(Submitted 28 October 1997)
Pis'ma Zh. Éksp. Teor. Fiz. **66**, No. 12, 765–770 (25 December 1997)

"Annealing" of sD_2 -influence on UCN yield - TRIGA

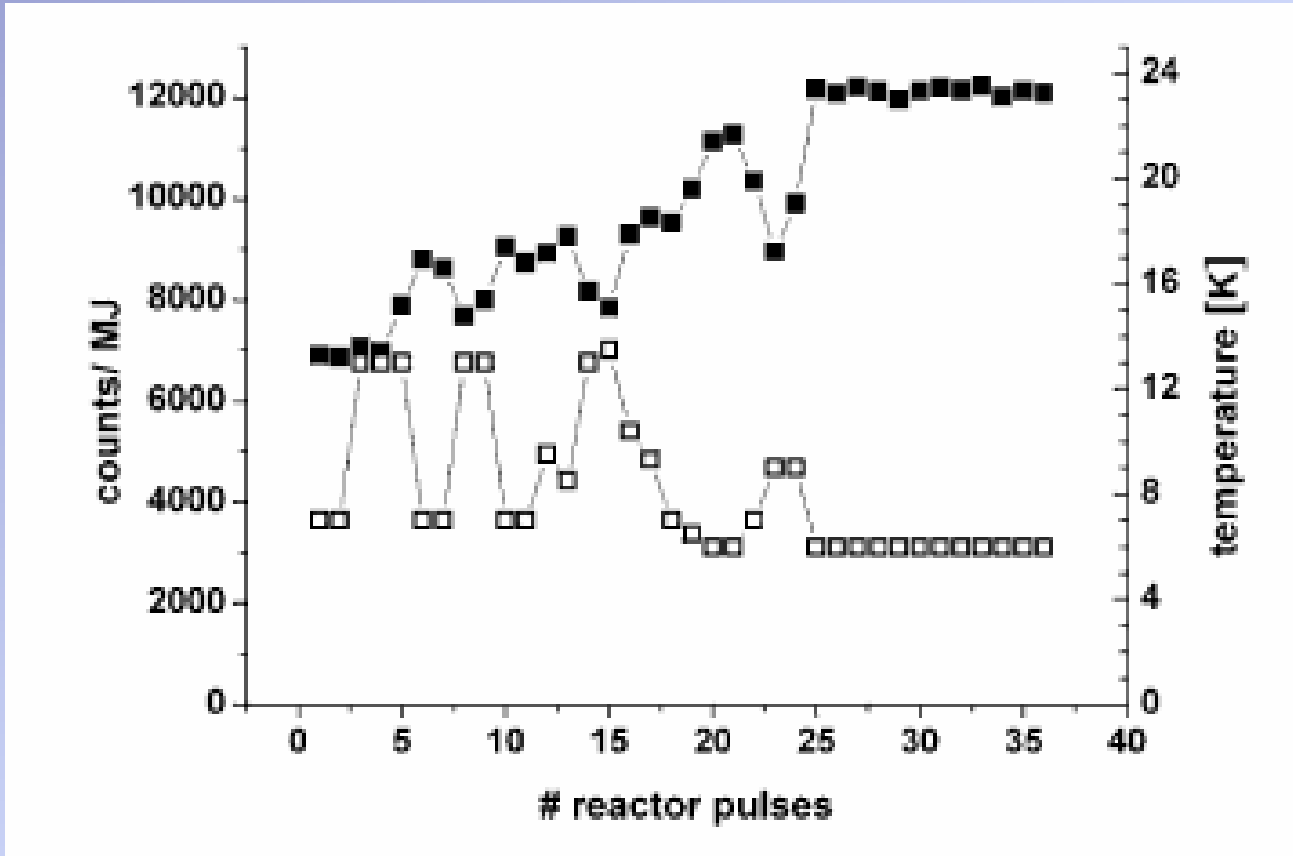

Gain ~ 70%

Annealing:

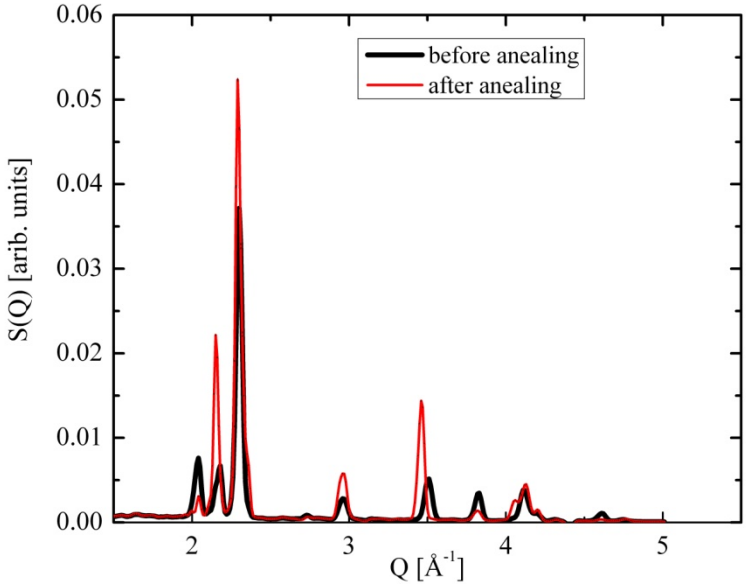
before anealing
after anealing
S(Q) [arib. units]
Q [Å^{-1}]
0.00
0.01
0.02
0.03
0.04
0.05
0.06
2
3
4
5

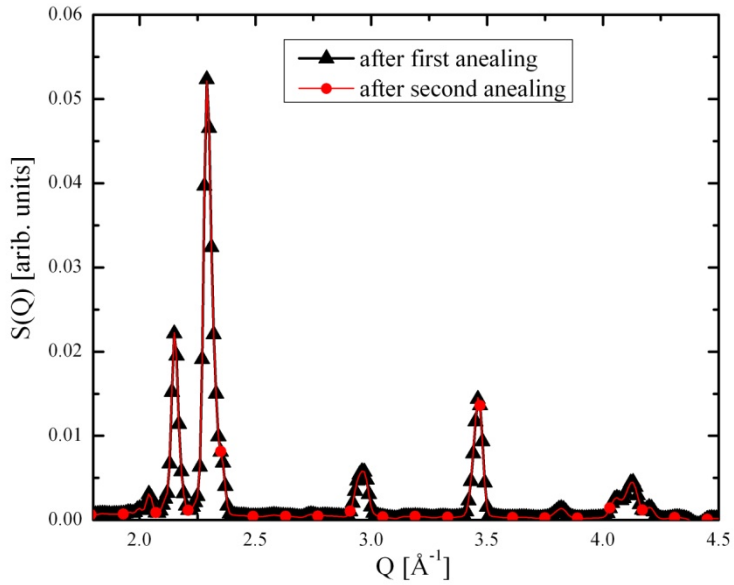
after first anealing
after second anealing
S(Q) [arib. units]
Q [Å^{-1}]
0.00
0.01
0.02
0.03
0.04
0.05
0.06
2.0
2.5
3.0
3.5
4.0
4.5

Inelastic UCN up-scattering:

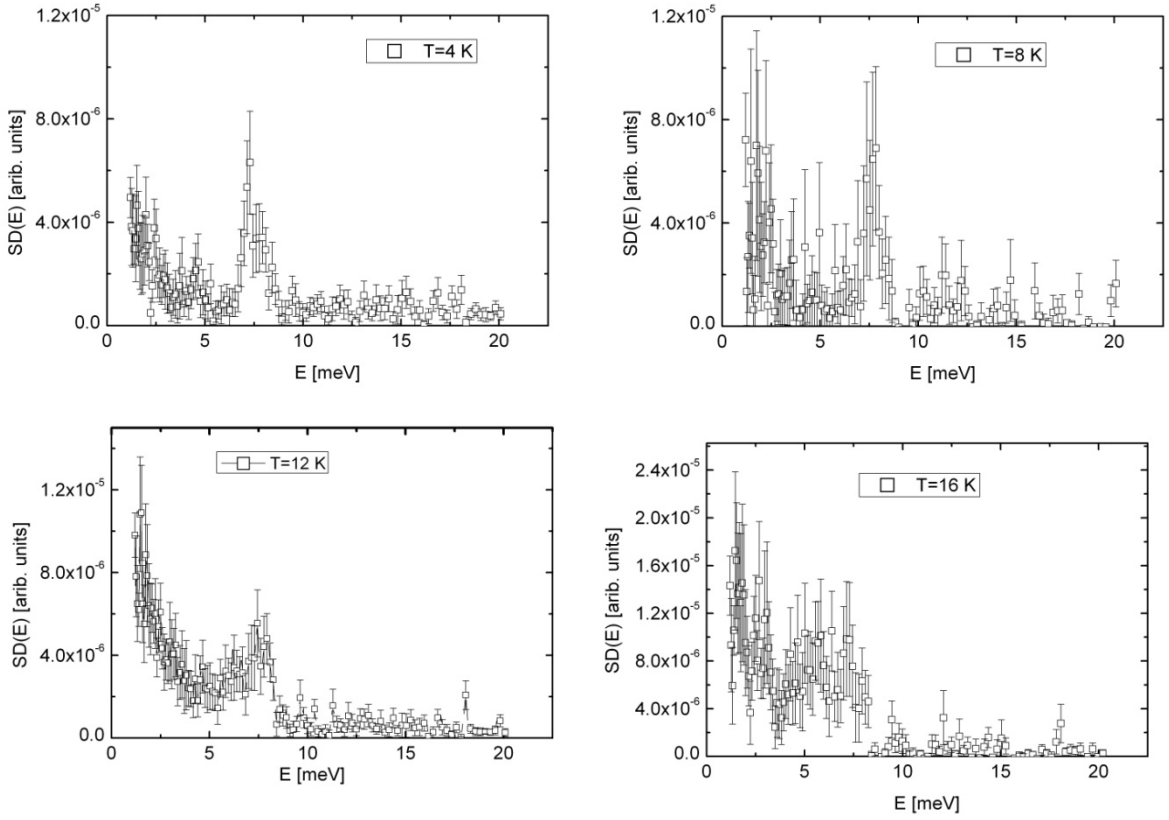

$$\sigma_{\rm loss}(E_i) = \frac{\sigma_0}{\sqrt{\frac{\hbar^2 E_i}{2m}}} \cdot \int_0^{E^{\rm max}} \sqrt{\frac{2mE}{\hbar^2}} S(\frac{2mE}{\hbar^2}, E) dE + \sigma_{inc}^{el}.$$

UCN loss cross section – temperature dependance

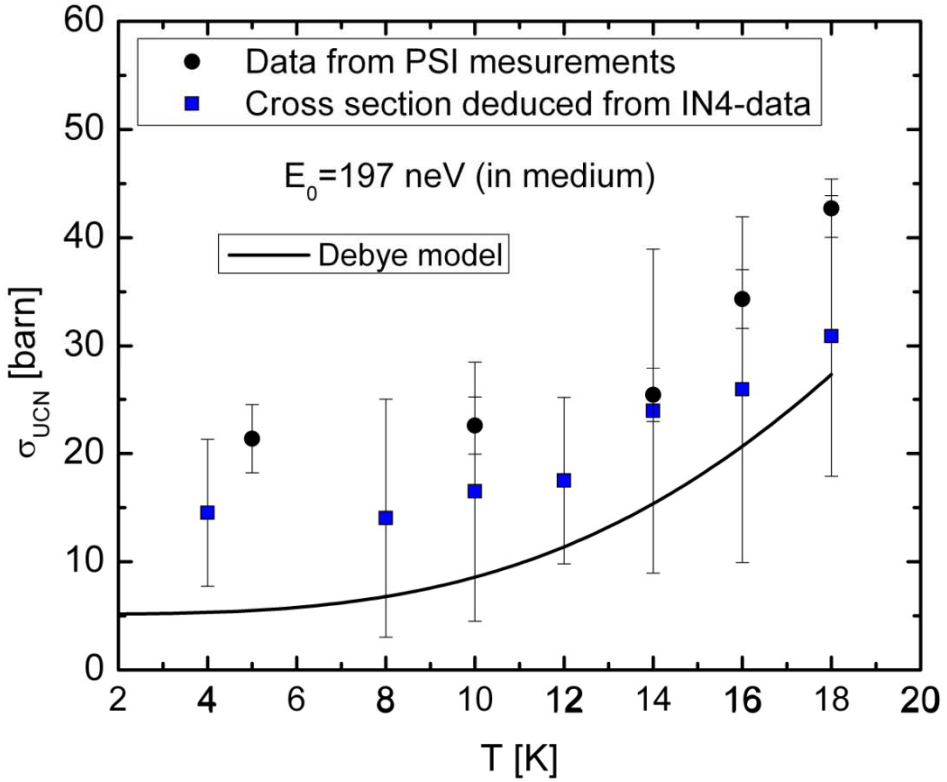

PSI-data: F. Atchison et al., PRL 95, 182502 (2005) and M. Kasprzak priv. communication

UCN loss cross section – energy dependance

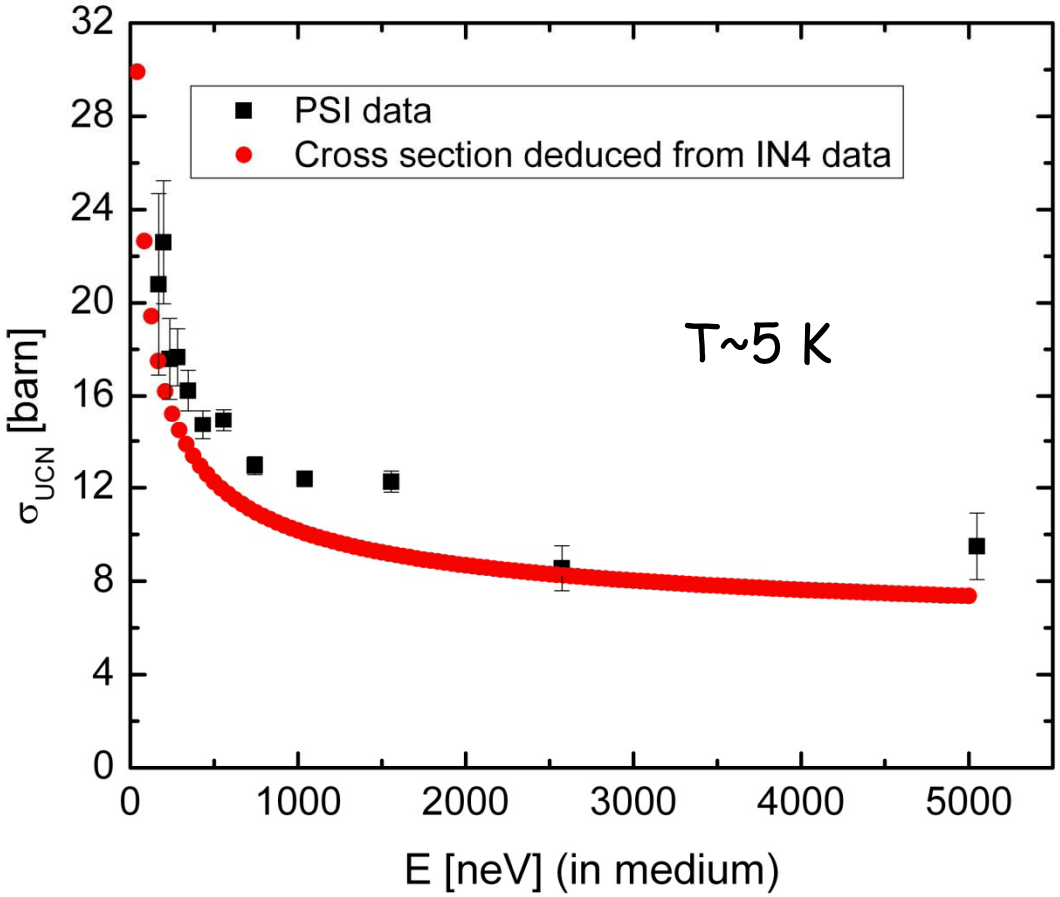

Mean free path of UCN

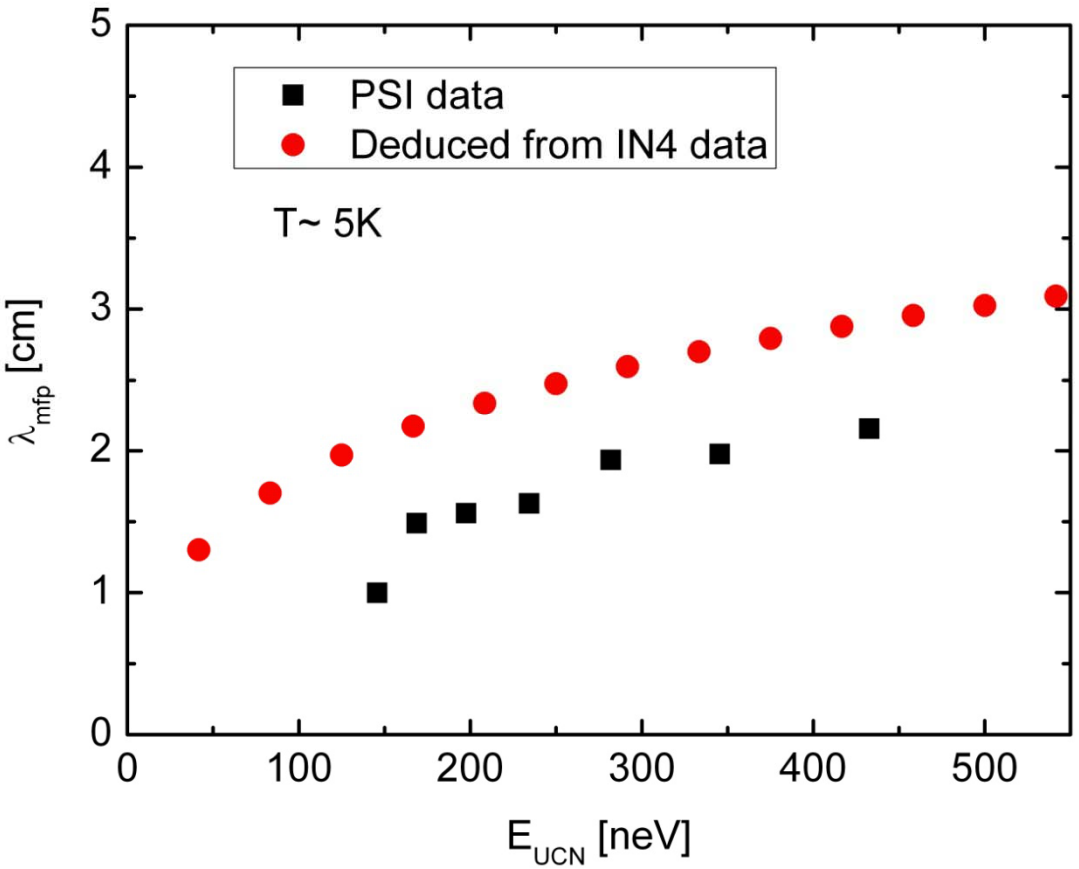

Possible theoretical explanations ?

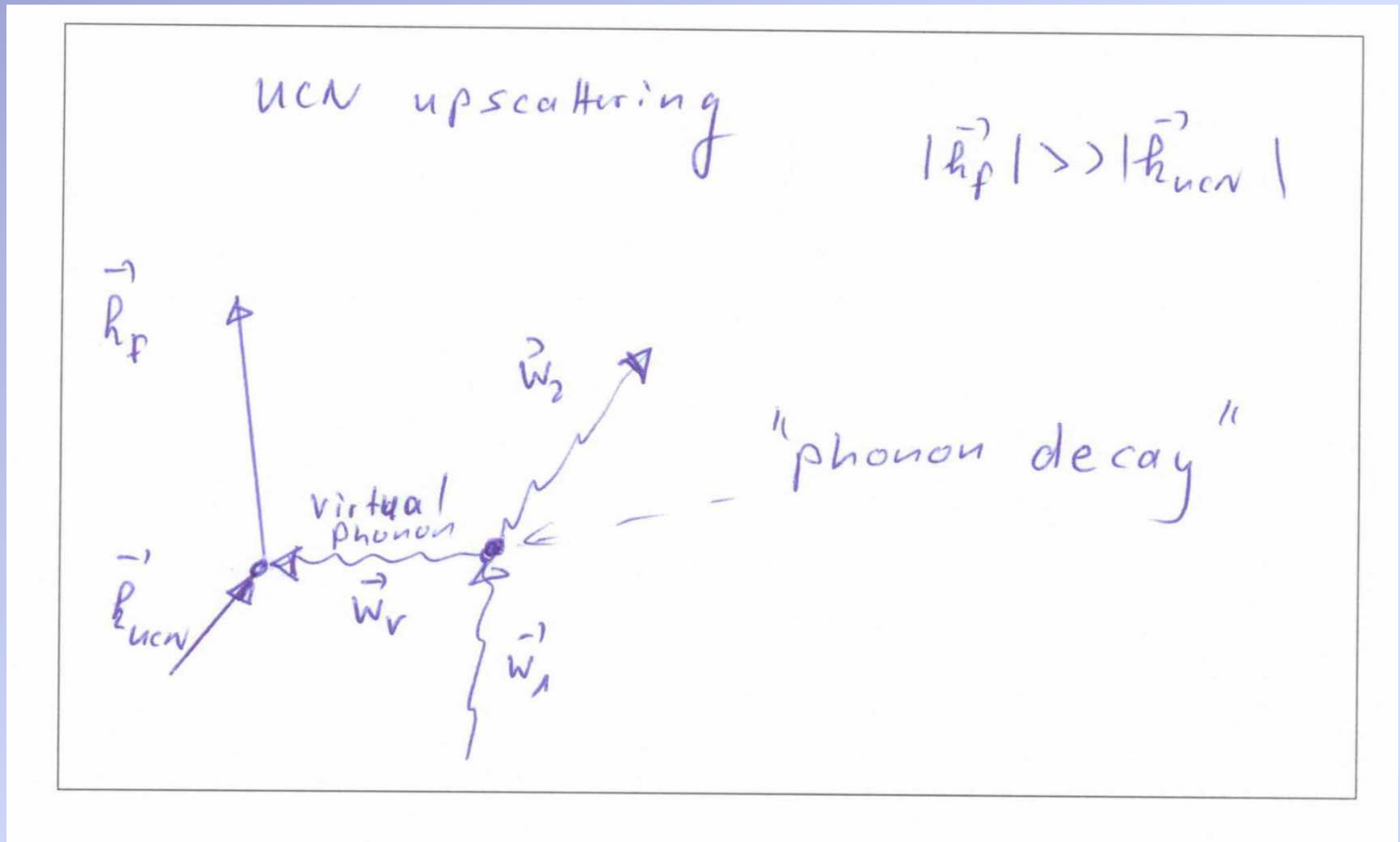

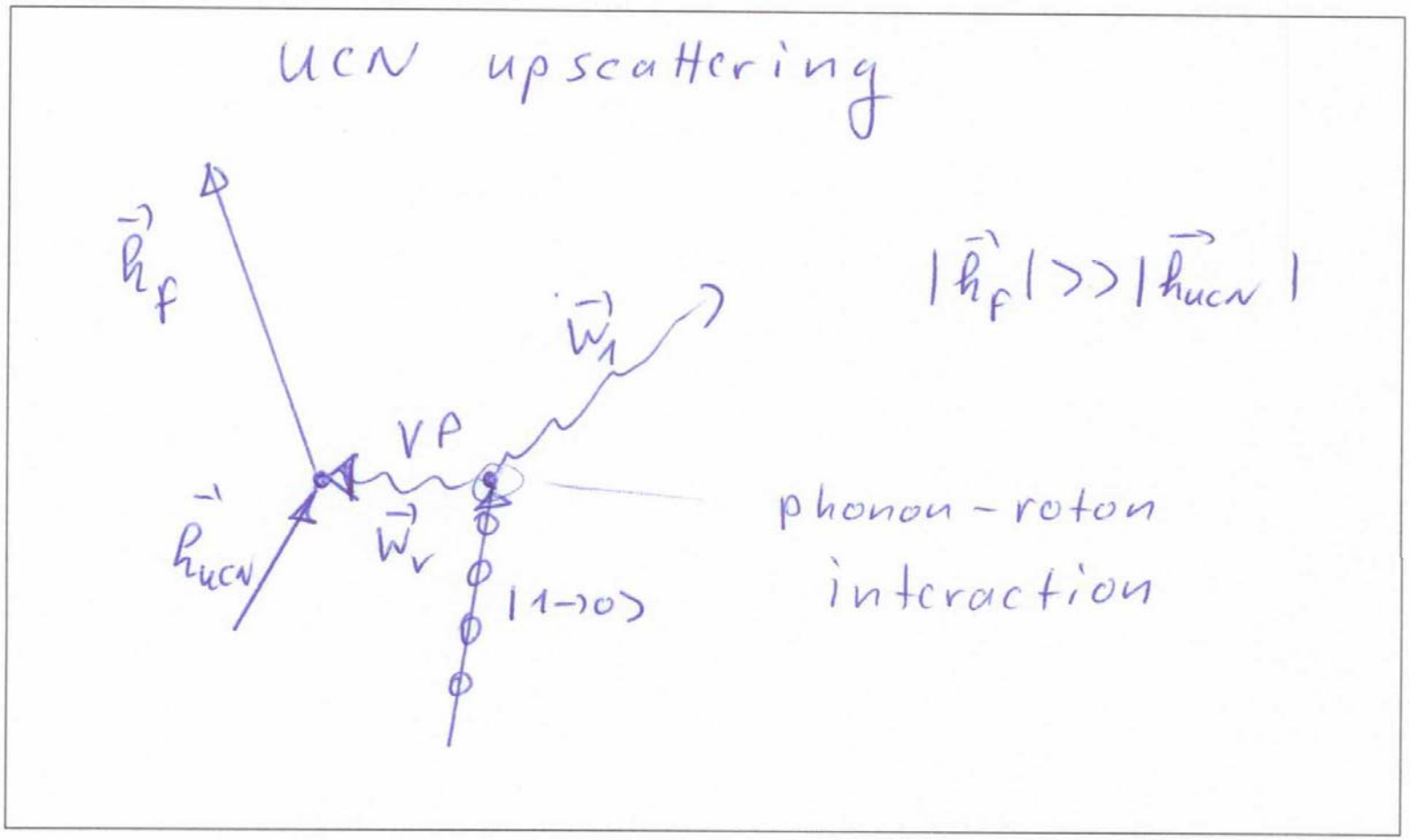
UCN upscattering
$\vec{k}_f$
$\vec{w}_1$
VP
$\vec{k}_{UCN}$
$\vec{w}_r$
|1→0>
$|\vec{k}_f| >> |\vec{k}_{UCN}|$
phonon - roton
interaction

Neutron scattering in solid α-oxygen (T<23 K)

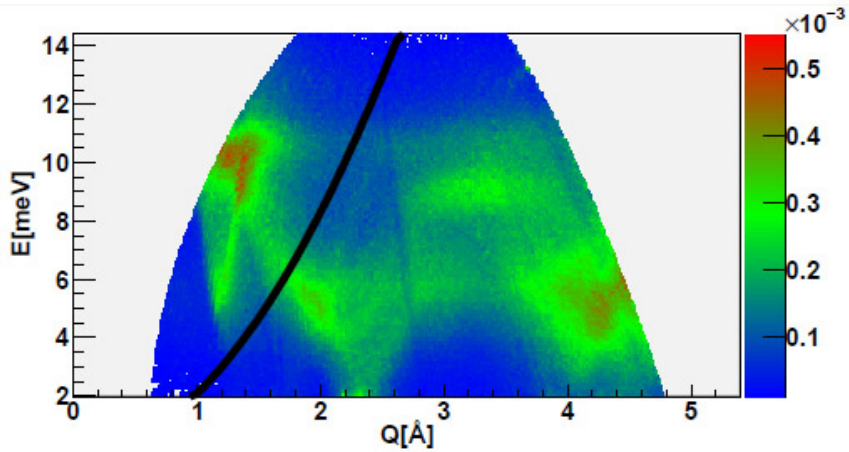

FIG. 1: $S(Q, E)$ of α-sO_2 at $T = 5$ K.
Data from IN4 measurements.
Black parabola: Dispersion of the free neutron.

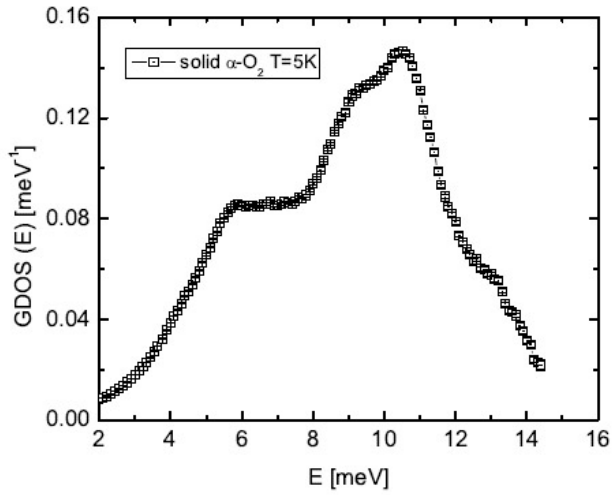

FIG. 2: Generalized density of states $GDOS(E)$ of α-sO_2 at $T = 5$ K.
Data from IN4 measurements.
GDOS is normalized to $\int_0^\infty GDOS(E) \cdot dE = 1$.

Calculated S(Q,ω) in α-O2

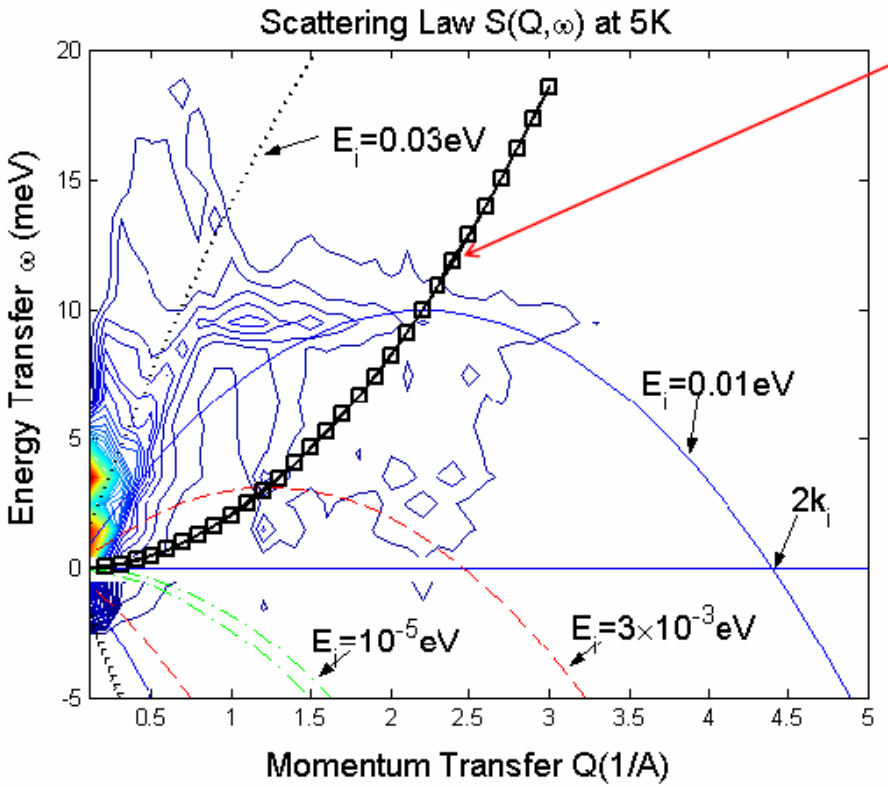

Free Neutron Dispersion Curve

Coupling constant

Suggested in P.W. Stephens and C.F. Majkrzak, Phys. Rev. B (1986)

J_{NN}=-2.44 meV
J_{NNN} = -1.22 meV

5

Chen-Yu Liu
June 8~14, 2009
7th International Workshop on Ultra Cold and Cold Neutrons Physics and Sources, St. Petersburg, Russia

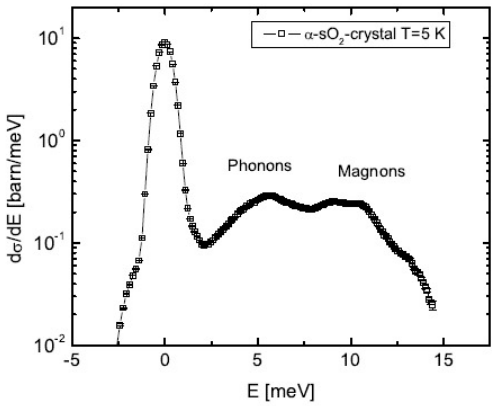

FIG. 3: $d\sigma/dE$ of α-sO_2 at $T = 5$ K. Data from IN4 measurements.

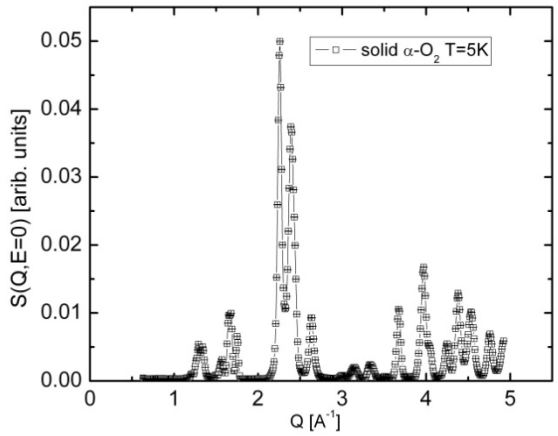

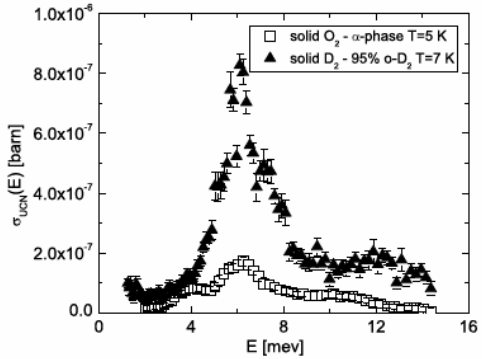

Fig. 4:
UCN production cross section of α-sO_2 ($\square$) at T =5 K and sD_2 (95% ortho concentration) ($\blacktriangle$) at $T = 7$ K [12]. UCN energy range 0-150 neV inside the solid D_2, UCN energy range 0-163 neV inside the solid α-sO_2. Cross sections determined by an integration of $S(Q, E)$ along the free dispersion of the neutron. Data from IN4 measurements.

UCN losses:

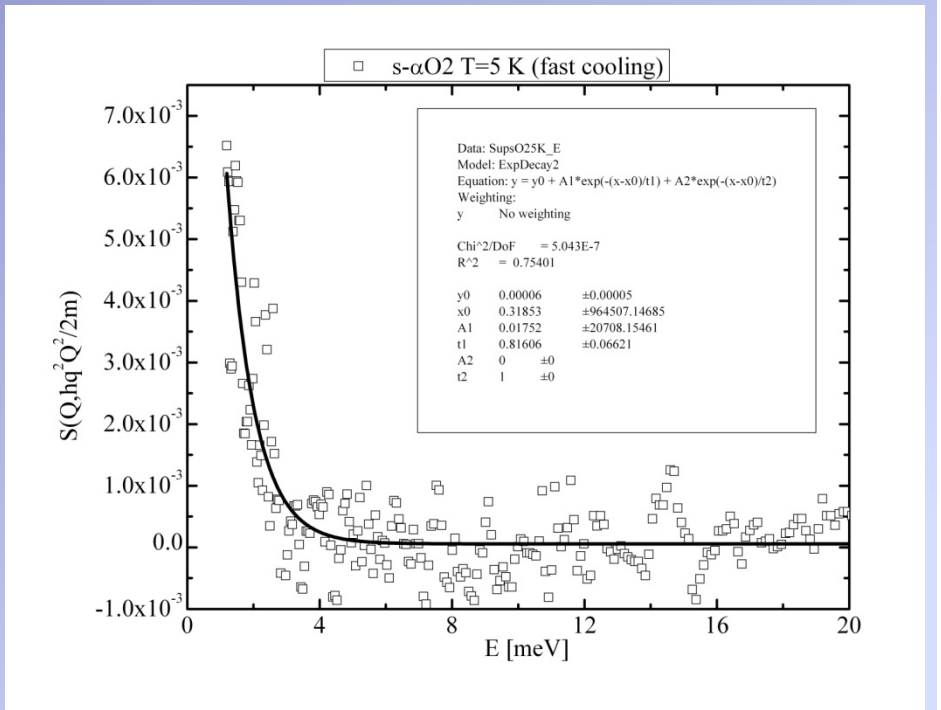
s-αO2 T=5 K (fast cooling)
Data: SupsO25K_E
Model: ExpDecay2
Equation: y = y0 + A1*exp(-(x-x0)/t1) + A2*exp(-(x-x0)/t2)
Weighting:
y No weighting
Chi^2/DoF = 5.043E-7
R^2 = 0.75401
y0 0.00006 ±0.00005
x0 0.31853 ±964507.14685
A1 0.01752 ±20708.15461
t1 0.81606 ±0.06621
A2 0 ±0
t2 1 ±0
S(Q,hq²Q²/2m)
E [meV]

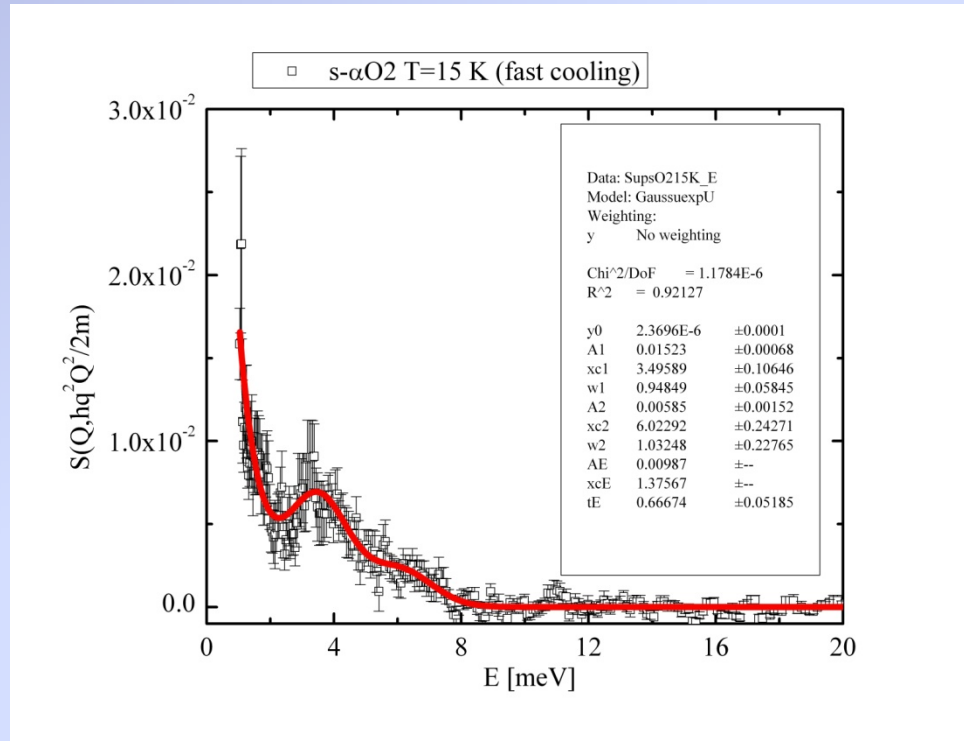
s-αO2 T=15 K (fast cooling)
Data: SupsO215K_E
Model: GaussuexpU
Weighting:
y No weighting
Chi^2/DoF = 1.1784E-6
R^2 = 0.92127
y0 2.3696E-6 ±0.0001
A1 0.01523 ±0.00068
xc1 3.49589 ±0.10646
w1 0.94849 ±0.05845
A2 0.00585 ±0.00152
xc2 6.02292 ±0.24271
w2 1.03248 ±0.22765
AE 0.00987 ±--
xcE 1.37567 ±--
tE 0.66674 ±0.05185
S(Q,hq²Q²/2m)
E [meV]

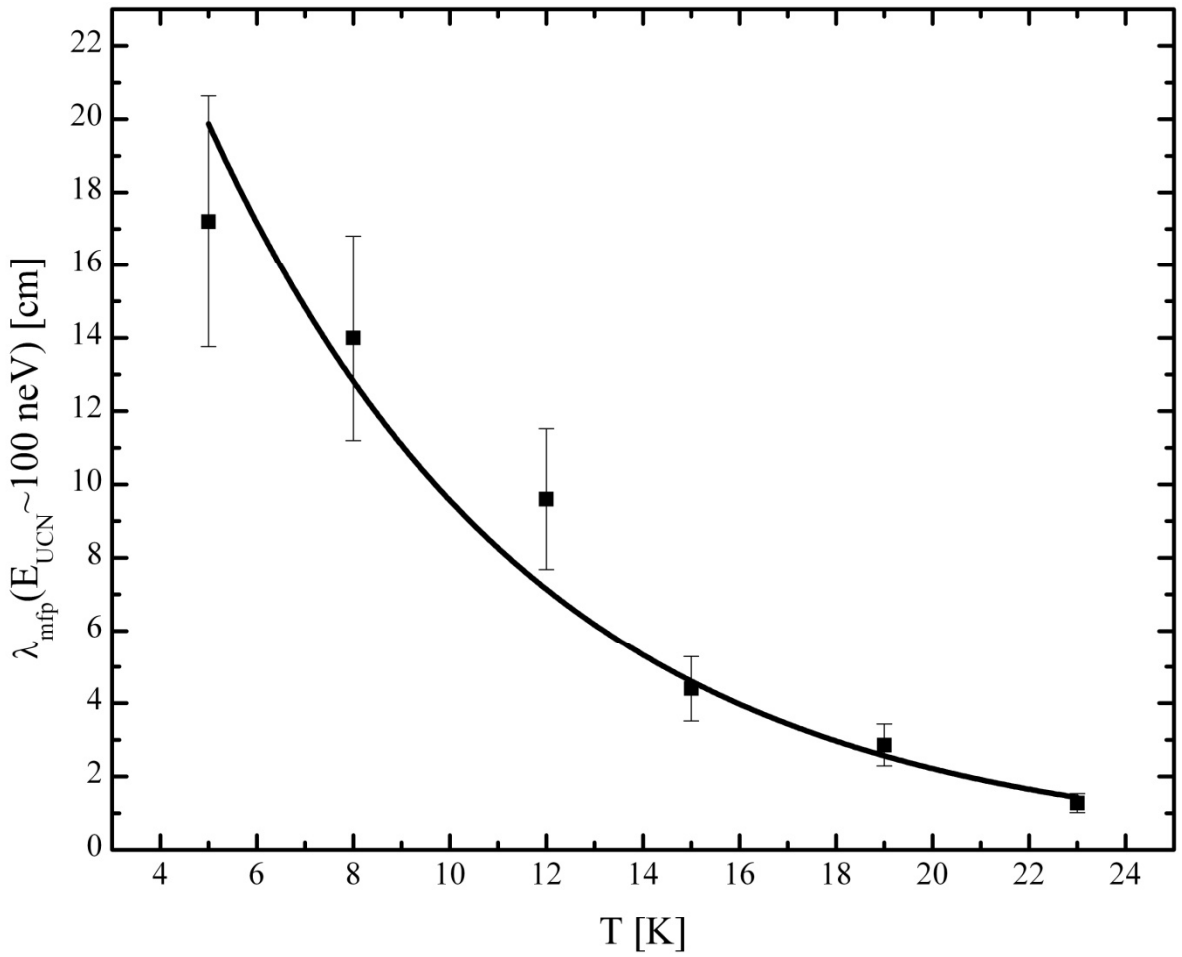
$\lambda_{mfp}(E_{UCN}\sim100$ neV) [cm]
T [K]
0
2
4
6
8
10
12
14
16
18
20
22
4
6
8
10
12
14
16
18
20
22
24

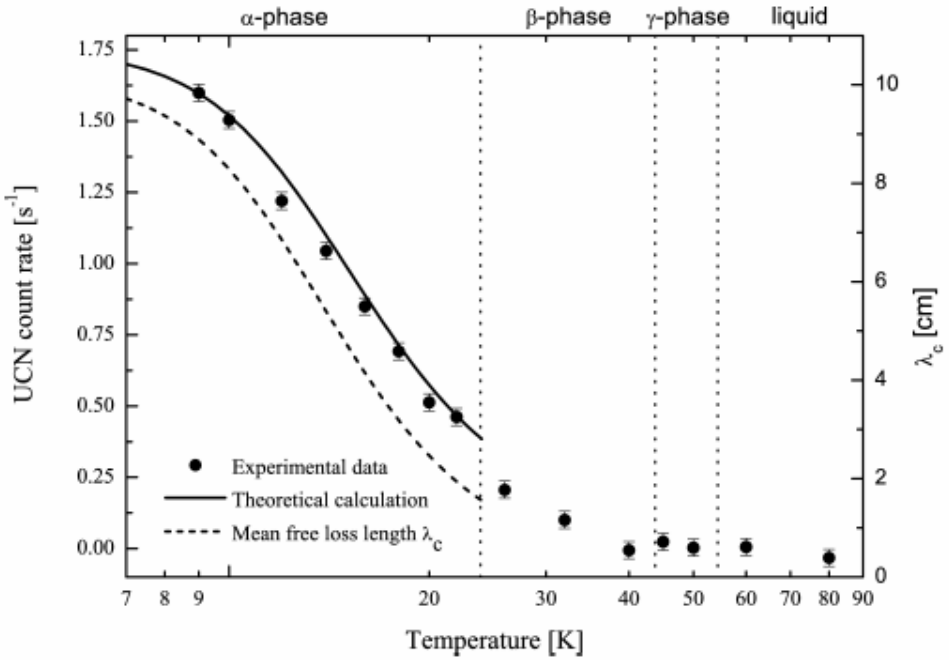

FIG. 3: Circles: Measured UCN count rates produced by a solid oxygen converter, depending on its temperature and solid state phase. Error bars indicate statistical uncertainties. Solid line: Calculated UCN count rate (see text for details). Dashed line: Mean free loss length λ_c (axis to the right) in the oxygen converter used for the calculations.

Summary

- First neutron scattering experiments on sD_2 and sO_2 delivers new data on the structure of the density of states in solid deuterium and oxygen
- It seems that sD_2 is a better converter for UCN production compared to sO_2
- The average neutron temperature of the incoming flux should be in the region of 40K for both converters
- Measured $S(q,\omega)$ can be used for UCN production calculation (no approximations !) as well for determination of UCN losses
- It seems, that the origin of UCN losses in sD_2 is purely inelastic
- Low energy and Q neutron scattering in sO2 would be helpful to study possible up-scattering of UCN through magnetic excitations.
- THANK YOU

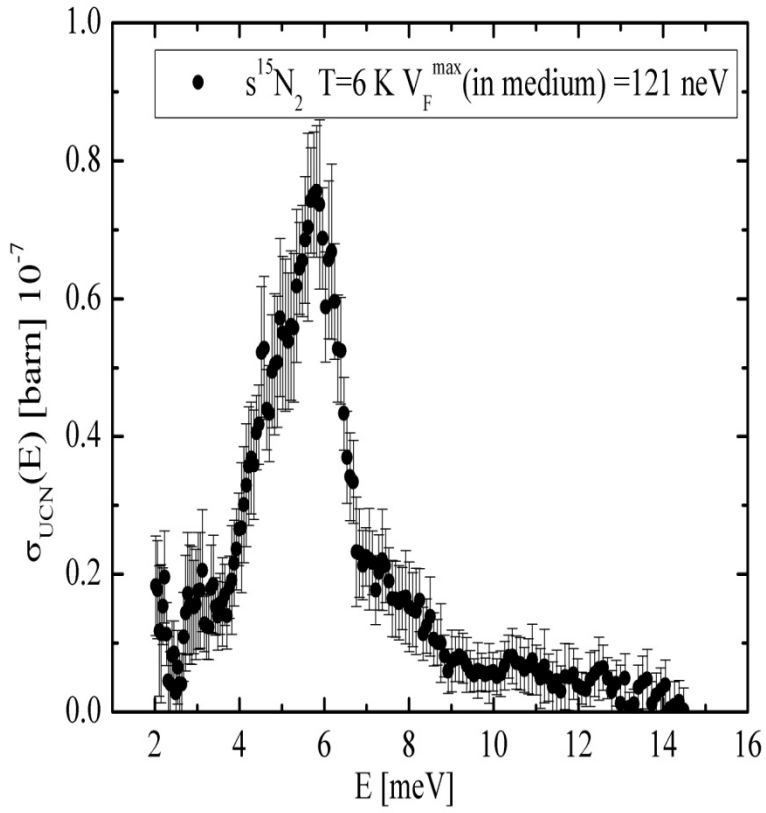
s15N2 T=6 K VF max(in medium) =121 neV
σUCN(E) [barn] 10-7
E [meV]
1.0
0.8
0.6
0.4
0.2
0.0
2
4
6
8
10
12
14
16

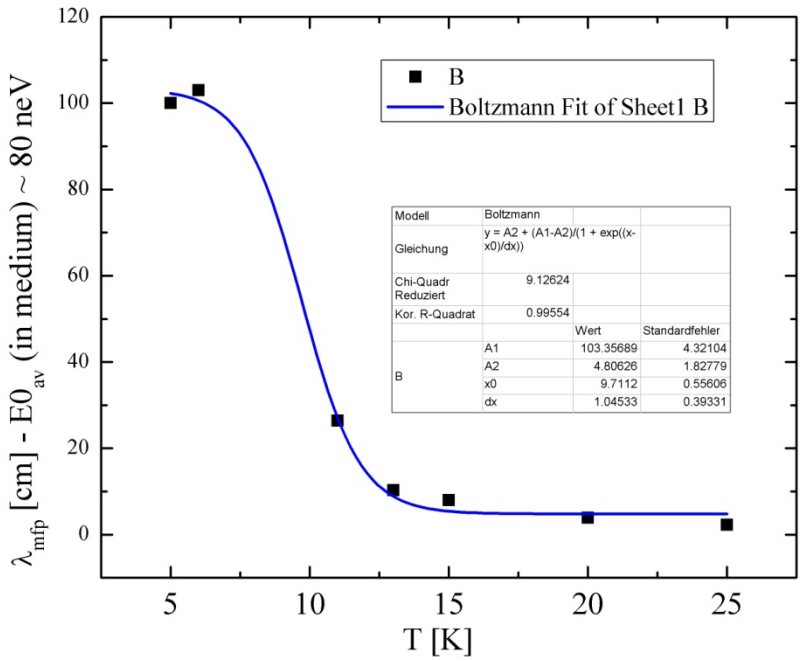
B
Boltzmann Fit of Sheet1 B
λmfp [cm] - E0av (in medium) ~ 80 neV
T [K]
120
100
80
60
40
20
0
5
10
15
20
25
Modell Boltzmann
Gleichung y = A2 + (A1-A2)/(1 + exp((x-x0)/dx))
Chi-Quadr Reduziert 9.12624
Kor. R-Quadrat 0.99554
Wert Standardfehler
B A1 103.35689 4.32104
A2 4.80626 1.82779
x0 9.7112 0.55606
dx 1.04533 0.39331